RECEIVER DESIGN FOR A CLASS OF NEW PULSE SHAPES FOR CPM SIGNALS

A THESIS SUBMITTED TO
THE GRADUATE SCHOOL OF NATURAL AND APPLIED SCIENCES
OF
MIDDLE EAST TECHNICAL UNIVERSITY

BY

BİLAL UĞURLU

IN PARTIAL FULFILLMENT OF THE REQUIREMENTS
FOR
THE DEGREE OF MASTER OF SCIENCE
IN
ELECTRICAL AND ELECTRONICS ENGINEERING

FEBRUARY 2012

Approval of the thesis:

RECEIVER DESIGN FOR A CLASS OF NEW PULSE SHAPES FOR CPM SIGNALS

submitted by **BİLAL UĞURLU** in partial fulfillment of the requirements for the degree of **Master of Science in Electrical and Electronics Engineering Department, Middle East Technical University** by,

Prof. Dr. Canan Özgen _____
Dean, Graduate School of **Natural and Applied Sciences**

Prof. Dr. İsmet Erkmen _____
Head of Department, **Electrical and Electronics Engineering**

Prof. Dr. Yalçın Tanık _____
Supervisor, **Electrical and Electronics Engineering Dept., METU**

Examining Committee Members:

Prof. Dr. Mete Severcan
Electrical and Electronics Engineering Dept., METU _____

Prof. Dr. Yalçın Tanık
Electrical and Electronics Engineering Dept., METU _____

Assoc. Prof. Dr. Melek Diker Yücel
Electrical and Electronics Engineering Dept., METU _____

Assoc. Prof. Dr. Ali Özgür Yılmaz
Electrical and Electronics Engineering Dept., METU _____

Çağdaş Enis Doyuran (M.Sc.)
Manager, ASELSAN _____

Date: _____

I hereby declare that all information in this document has been obtained and presented in accordance with academic rules and ethical conduct. I also declare that, as required by these rules and conduct, I have fully cited and referenced all material and results that are not original to this work.

Name, Last Name: BİLAL UĞURLU

Signature :

ABSTRACT

RECEIVER DESIGN FOR A CLASS OF NEW PULSE SHAPES FOR CPM SIGNALS

Uğurlu, Bilal
M.Sc., Department of Electrical and Electronics Engineering
Supervisor : Prof. Dr. Yalçın Tanık

February 2012, 69 pages

Recently, a study on obtaining better Euclidean distance for CPM (Continuous Phase Modulation) signals that fit well-known GSM spectral envelope has been carried out, and significant performance improvements were obtained. Two new pulse shapes, which are represented using 8^{th} degree polynomials, were optimized to give the best error performance under the constraint that the PSD stays below GSM spectral standards. However, the approach uses parameters that cause the number of states to increase considerably, and thus yielding high complexity for receiver implementation. In this thesis, a study on finding a feasible receiver design that can provide a performance with acceptable degradation but affordable complexity is carried out for those new pulse shapes. After a survey about complexity reduction techniques, a decision is made to go on with a receiver structure based on Laurent Decomposition (LD) of phase modulated signals. Unlike other complexity reduction techniques, usage of LD based receivers permits reduction in both the number of matched filters and trellis states. Throughout the study, different numbers of matched filters and trellis states were used in LD based receivers for the new pulse shapes, and good results are obtained. For the pulse shape with pulse length $L = 3$, about a gain of 0.93dB in power is achieved by only 2 matched filters and 14 trellis states. For the case where $L = 7$, approximately a gain of 2.25dB is achieved with only 8 matched filters and 56 states, whereas 896 matched filters and 448 states

are needed in the optimum case without complexity reduction.

Keywords: Continuous Phase Modulation (CPM), Laurent Decomposition, Maximum Likelihood Sequence Estimation (MLSE), Reduced-Complexity CPM Receiver, Global System for Mobile Communications (GSM)

ÖZ

SÜREKLİ FAZ MODÜLASYONLU SİNYALLER İÇİN GELİŞTİRİLMİŞ BİR GRUP YENİ DARBE ŞEKİLLERİ İÇİN ALMAÇ TASARIMI

Uğurlu, Bilal
Yüksek Lisans, Elektrik ve Elektronik Mühendisliği Bölümü
Tez Yöneticisi : Prof. Dr. Yalçın Tanık

Şubat 2012, 69 sayfa

Geçtiğimiz yıllarda, GSM spektral zarfına iyi uyum sağlayan CPM (Sürekli Faz Modülasyonu) sinyaller için daha iyi Öklit uzaklığı elde edilmesi üzerine bir çalışma yapılmış, ve bu konuda kayda değer performans iyileştirmeleri sağlanmıştır. Güç spektral yoğunlukları GSM spektral standartlarına uymak kaydıyla, 8. dereceden polinomlar kullanılarak oluşturulan iki yeni darbe şekli, en iyi hata performansını verecek şekilde optimize edilmiştir. Ancak bu yaklaşım, durum sayısında dikkate değer bir artışa neden olabilecek parametreler kullanmakta, ve böylece almaç yapımında yüksek karmaşıklığa yol açmaktadır. Bu tezde, bu darbe şekilleri için yeterince indirgenmiş ve uğraşılabilir bir karmaşıklığa sahip, iyi performans sağlayabilecek, uygulanabilirliği yüksek bir almaç tasarımı bulmaya yönelik çalışma yapılmıştır. Karmaşıklık azaltma teknikleri incelendikten sonra, faz modülasyonlu sinyallerin Laurent ayrışımına (LD) dayalı bir almaç yapısı ile yola devam edilmeye karar verilmiştir. Diğer karmaşıklık azaltma tekniklerinin aksine, LD tabanlı almaçlar hem kullanılan uyumlu süzgeç hem de durum sayısının azaltılabilmesine izin vermektedir. Çalışma boyunca, yeni darbe şekilleri için geliştirilen LD tabanlı almaçlarda farklı süzgeç ve durum sayıları kullanılmış ve iyi sonuçlar elde edilmiştir. Darbe uzunluğu $L = 3$ olan darbe şekli için, sadece 2 uyumlu süzgeç ve 14 durum kullanılarak, 0.93dB civarında bir güç kazancı

elde edilmiştir. $L = 7$ durumu için ise, karmaşıklık azaltma uygulanmadan önce optimum almaçta 896 süzgeç ve 448 durum sayısı gerekirken, sadece 8 uyumlu süzgeç ve 56 durum kullanılarak yaklaşık 2.25dB'lik bir kazanç sağlanmıştır.

Anahtar Kelimeler: Sürekli Faz Modülasyonu (CPM), Laurent Ayrışımı, En Büyük Olabilirlik Dizi Kestirimi (MLSE), Azaltılmış Karmaşıklıkta CPM Almacı, Mobil İletişim için Evrensel Sistem (GSM)

To my family,

ACKNOWLEDGMENTS

I would like to express my deepest gratitude to my supervisor Prof. Dr. Yalçın Tanık for his encouragements, guidance, advices, criticism and insight throughout the research. My vision about telecommunications has broadened by his helps.

I would also like to express my thanks to Ç. Enis Doyuran for his suggestions, comments and invaluable helps.

I would like to forward my appreciation to all my friends and colleagues who contributed to my thesis with their continuous encouragement.

I am deeply grateful to ASELSAN Inc. for letting me involve in this thesis study. Additionally, I want to express my thanks to TÜBİTAK BİDEB and TURKCELL AKADEMİ for their financial support during my thesis research.

I would like to express my very special thanks to my family for their great patience, understanding, morale support and endless love. They have always encouraged and supported me in my entire life.

Finally, I would like to thank anybody that I might have mistakenly disregarded.

TABLE OF CONTENTS

LIST OF TABLES

TABLES

LIST OF FIGURES

FIGURES

CHAPTER 1

INTRODUCTION

1.1 SCOPE AND OBJECTIVE

In digital communication systems, continuous phase modulation (CPM) is very popular because of its gorgeous spectral properties and good error probability. Especially in mobile communications, CPM is employed in several communication standards like GSM, DECT, Bluetooth etc. Its constant envelope nature makes it very attractive for wireless media, where nonlinear amplifiers are preferably used for higher efficiency in power. Since it is a nonlinear modulation scheme, the performance of CPM is not affected by nonlinear operations involved by transmitters.

In July 2001, an M.Sc. thesis has been carried out [5], about obtaining better Euclidean distance for CPM signals under the constraint that the power spectral density should stay below the GSM spectral envelope, by Ç. E. Doyuran. This goal has been realized by finding new pulse shapes based on polynomial approach, and significant performance improvements were obtained. However, the signal parameters realizing the objective of this study cause considerable increment in the number of states and matched filters at the receiver side, which results in receiver complexity. In the mentioned study, this situation is not considered. Therefore, a need for a new study on receiver structures which can provide a performance with acceptable degradation but affordable complexity has emerged. In this thesis, we are looking for the ways to reduce the complexity of the receiver needed for these new pulse shapes without sacrificing the improvements in their error performances.

In continuous phase modulation schemes, the receiver complexity increases exponentially as the memory introduced to the system is increased. CPM memory directly depends on the length of the *baseband shaping pulse* (or *frequency pulse*) and the modulation index employed in the system. As the length of the pulse shape increases, more pulses begin to overlap which results in more *correlative states* to be handled by the receiver. And the value of the modulation index determines the number of *phase states*. More states means more complex decoder implementations and more matched filters to be designed.

Receiver complexity problem can be divided into two parts: matched filter complexity and decoding stage (trellis states) complexity. There have been several studies and important progress on both areas. In matched filter complexity reduction area, the objective of most studies was finding a set of orthonormal basis functions to use instead of matched filters, and implement a limited number of these functions in the receiver to reduce the number of filters used. In [16], derivation of orthonormal basis functions is accomplished by using Gram-Schmidt orthogonalization procedure. Sampling functions are used in [18] to obtain the desired functions. There have been an approach with Walsh functions in [14] for the same purpose. However, usage of limited basis functions in all of these proposed receivers lead to a trade-off between the complexity and performance, and no reduction in trellis state numbers is achieved.

In the area of decoding stage complexity reduction, which means reducing the number of trellis states, there have been some studies, too. In [19], a decoder using a reduced search algorithm without any reduction on trellis structure is proposed, whereas in [13], a reduced state sequence detection method running on a smaller trellis with the usage of decision feedback is developed. However, in these last two detectors the number of matched filters remain unchanged.

There also have been some studies about complexity reduction techniques in both matched filter and state numbers. In [17] a method that truncates the baseband shaping pulse to a smaller length for the receiver side is proposed. Since the length of the pulse shape that the detector is based on is smaller than the one used in the transmitter side, the detector is called

a *mismatched detector*. Mismatch detector usage reduces both trellis state and matched filter numbers, but degradation in performance is observed.

One of the most attractive works conducted in this area is the paper published by Pierre A. Laurent, which is found to be very useful in the literature and has a lot of citations. In his paper, [7], Laurent shows that a binary CPM signal can be exactly constructed by linear superposition of amplitude modulated signals. The nonlinear nature of CPM is reserved by the nonlinear coefficients applied to the pulses, which are created by the data bits. The energy is not distributed evenly among these PAM waveforms, so excluding the ones with little energy from the linear combination does not cause a noticeable degradation; in some cases the performance is almost the same with the optimal case. In a receiver adopting Laurent decomposition technique, matched filters are just the time inverse of the PAM waveforms that construct the transmitted signal. Hence excluding some of these pulses directly reduces the number of matched filters, and the number of states because of the decrement in the number of coefficients too. By using Laurent decomposition method, large complexity reductions can be achieved by almost no degradation in error performance.

In this work, we adopt complexity reduction techniques that uses Laurent decomposition method since both the number of matched filters and trellis states is large for the pulse shapes derived in [5].

1.2 OUTLINE OF THE THESIS

In Chapter 2, continuous phase modulation (CPM) is summarized briefly. First the standard signal definition is given, followed by the signalling types used in CPM. After the standard definition, the PAM representation of CPM, which is also known as the Laurent Decomposition is expressed briefly.

In Chapter 3, the coherent receiver structures used for the reception of continuous phase modulated signals is presented. The chapter starts with the definitions of the optimum maximum likelihood sequence estimating (MLSE) receiver structure based on phase trellis, and ends

with the receiver structure based on Laurent decomposition of CPM signals, which has less matched filters and encourages state reduction in the Viterbi decoder part.

In Chapter 4, the subject is about some new spectrally efficient pulse shapes having attractive error performances, which have been studied in an M.Sc. Thesis by Ç. Enis Doyuran in 2001. First the criteria to search and measure the quality of the new pulse shapes, which are the power spectral density and minimum Euclidean distance, are discussed briefly. The methods used for calculating these parameters are explained. The chapter ends with a summary of the polynomial approach used in the work to form new pulse shapes.

In Chapter 5, proposed receivers and the simulations conducted to measure the error performance of the proposed receivers are explained. First, information about the transmitter, channel and the receiver models used in simulations is given. It is followed by the verification of these models with MSK signaling scheme. Then a section illustrating the error performance of the optimum CPM receiver for the GMSK signal used in GSM is presented. Lastly, the proposed receivers for the new pulse shapes of [5] and their simulation results are given at the end of the chapter.

Finally, in Chapter 6, conclusions about this work are stated.

CHAPTER 2

REVIEW OF CONTINUOUS PHASE MODULATION

2.1 INTRODUCTION

The main purpose of the communications discipline is transmission of data in any medium as *reliably* as it can be achieved. But it is not so easy to create a reliable communication link to achieve the desired error probabilities, especially when we talk about wireless communications where the channels are strictly bandlimited. Living in a world where the resources for data transmission are not unlimited pushes communications design engineers into a survey where bandwidth and power efficiency is a big challenge that must be overcome. Regarding these constraints, continuous phase modulation signaling schemes has gained a growing interest in the last decades.

Continuous phase modulation (CPM) owes its widespread use to its two favorable characteristics. Having no amplitude variations in the transmitted signal, which makes it a *constant envelope* signal, is the first one. Usage of constant envelope modulation schemes is a necessity in applications where power supply constraints forces the use of saturated nonlinear amplifiers. Simple and low-cost transmitters are also other applications where constant envelope modulations are useful. The second favorable characteristic of continuous phase modulation is bandwidth and power efficiency. The CPM signal to be used can be adjusted to have the desired power and bandwidth properties with three parameters. These are the size of the data alphabet, the modulation index (or indices, if more than one will be used), and the length and shape of the frequency pulse. One can control the minimum Euclidean distance, which affects the power efficiency, and spectrum of the signal by selecting these

three properties carefully. We can conclude that continuous phase modulation (CPM) is a *constant envelope, nonlinear* modulation scheme with *attractive spectral properties* [5, 9], which makes it so popular in digital communications.

In this chapter, a review of continuous phase modulation is presented; including the standard CPM signal definition, signaling schemes that are used, phase trellis concept and signal state definition, and Laurent decomposition of CPM signals which serves to represent them as a linear sum of amplitude modulated pulses. A more detailed treatment of continuous phase modulation can be found in [1, 2, 3, 7]

2.2 CPM SIGNAL MODEL

In continuous phase modulation, the digital information is carried in the phase of the carrier signal. The data symbols modulate the instantaneous phase of the carrier and phase variation is continuous in time, hence the name *continuous phase* modulation is given.

2.2.1 STANDARD SIGNAL NOTATION

In a communications system employing continuous phase modulation, the transmitted signal is represented as in the following equation [1],

$$s(t,\overline{\alpha}) = \sqrt{\frac{2E_s}{T}}\cos\left[2\pi f_c t + \phi(t,\overline{\alpha}) + \phi_0\right] \tag{2.1}$$

where E_s is the symbol energy, T is the period, f_c is the carrier frequency, $\phi(t,\overline{\alpha})$ is the information-bearing phase which is a continuous function of time, and ϕ_0 is an arbitrary constant phase offset which can be set to zero implying that the system is coherent, without loss of generality. The information data sequence $\overline{\alpha} = \cdots, \alpha_{-2}, \alpha_{-1}, \alpha_0, \alpha_1, \alpha_2, \cdots$ that affects the phase $\phi(t,\overline{\alpha})$, causing it to change with time, is theoretically an infinitely long sequence of $M-$ary data symbols which are independent and identically distributed. Each data symbol takes one of the values

$$\alpha_k = \pm 1, \pm 3, \cdots, \pm(M-1), \qquad \text{where } k = \cdots, -2, -1, 0, 1, 2, \cdots$$

with equal probability $1/M$.

Looking at the equation (2.1), the constant envelope, nonlinear nature of the CPM signal can easily be seen. Regardless of the data, the amplitude, $\sqrt{2E_s/T}$, of the envelope of the transmitted signal is constant. Since the information is carried within the carrier phase, this makes the modulation scheme nonlinear.

The data sequence $\overline{\alpha}$ modulates the information-bearing phase of the transmitted signal according to

$$\phi(t, \overline{\alpha}) = 2\pi \sum_{k=-\infty}^{\infty} \alpha_k h_{\underline{k}} \int_{-\infty}^{t} g(\tau - kT) d\tau \tag{2.2}$$

where α_k is the data affecting the phase in the kth symbol duration, $h_{\underline{k}}$ is the kth *modulation index* which is a member of the sequence $\overline{h} = \cdots, h_{-2}, h_{-1}, h_0, h_1, h_2, \cdots$ of modulation indices, and $g(t)$ is the *baseband shaping pulse*. The baseband shaping pulse affects the instantaneous frequency of the transmitted signal, hence the name *frequency pulse* is also used widely for $g(t)$.

In equation (2.2), the subscript of the modulation index is shown with a bar below, which indicates that it is chosen from a predetermined set of H different modulation indices in a cyclic fashion. This means that $h_{\underline{k}}$ appears modulo H, and thus $\underline{k} = k \bmod H$. When $H = 1$, which is the most common case, only one modulation index exists that is denoted only h, with no subscripts. In this work, only the cases employing one modulation index are studied.

The baseband shaping pulse $g(t)$ must be of finite duration occupying $[0, LT]$, lasting for one or more symbol periods according to the value of L, and chosen such that it integrates to $1/2$ for normalization purposes. Since the baseband shaping pulse does not directly affect the phase, but its time integral does, a new pulse directly affecting the phase of the transmitted signal can be defined as,

$$q(t) = \int_{-\infty}^{t} g(\tau) d\tau \tag{2.3}$$

which is called the *phase pulse* or the *phase smoothing response* of the transmitted CPM signal. The goal of the normalization procedure that forces the frequency pulse $g(t)$ to integrate to $1/2$ is to set $q(LT) = 1/2$ and hence allow the maximum absolute phase change over one symbol interval to be $(M-1)h\pi$. Now equation (2.2) can be reexpressed as,

$$\phi(t, \overline{\alpha}) = 2\pi h \sum_{k=-\infty}^{\infty} \alpha_k q(\tau - kT) \tag{2.4}$$

where $H = 1$ is assumed for the modulation index.

2.2.2 SIGNALING TYPES OF CPM

Two types of signaling schemes exist for systems employing continuous phase modulation. This classification is made by considering the length of the baseband shaping pulse $g(t)$.

2.2.2.1 FULL RESPONSE SYSTEMS

If the duration of the baseband shaping pulse $g(t)$ is equal to only one symbol period, namely $L = 1$, then each data symbol affects the instantaneous frequency of the transmitted signal in only one symbol interval. Hence, the phase smoothing response $q(t)$ also reaches its final value $1/2$ in one symbol period.

For illustration, a rectangular and a raised cosine baseband shaping pulses are given with the corresponding phase smoothing responses in figures 2.1 and 2.2. The equation for the full response rectangular pulse is,

$$g(t) = \begin{cases} \dfrac{1}{2T} & 0 \le t \le T \\ 0 & otherwise \end{cases} \tag{2.5}$$

and the equation for the full response raised cosine pulse is,

$$g(t) = \begin{cases} \dfrac{1}{2T}\left[1 - \cos\dfrac{2\pi t}{T}\right] & 0 \le t \le T \\ 0 & otherwise \end{cases} \tag{2.6}$$

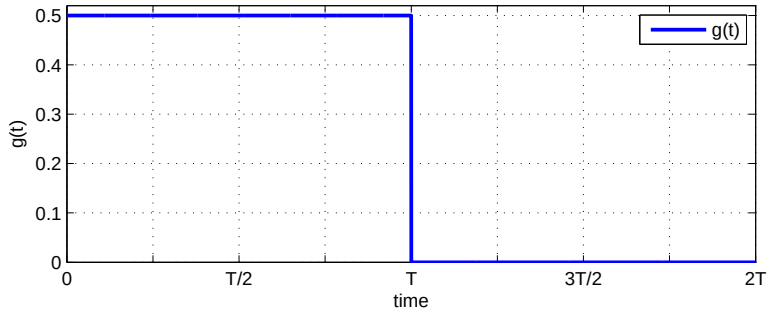

(a) Frequency Pulse

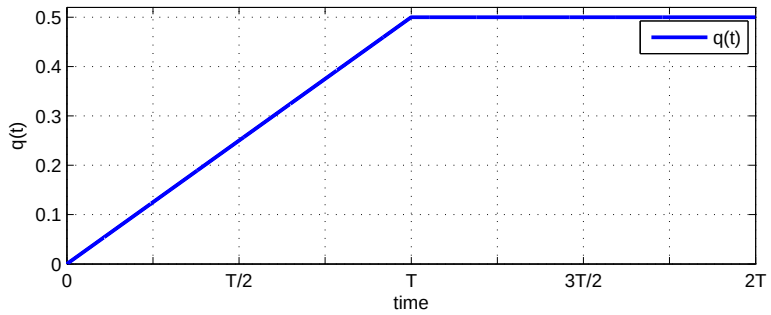

(b) Phase Smoothing Pulse

Figure 2.1: Full Response Rectangular Pulse (L = 1)

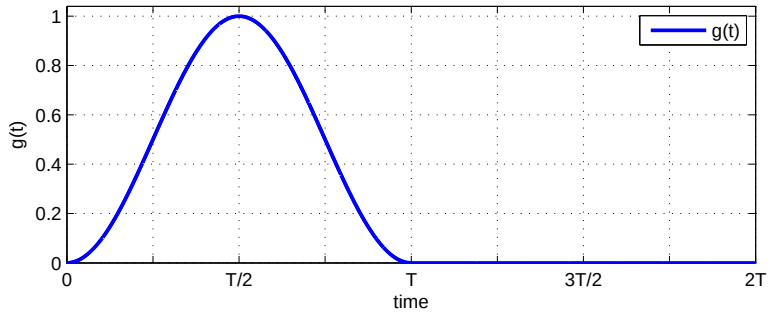

(a) Frequency Pulse

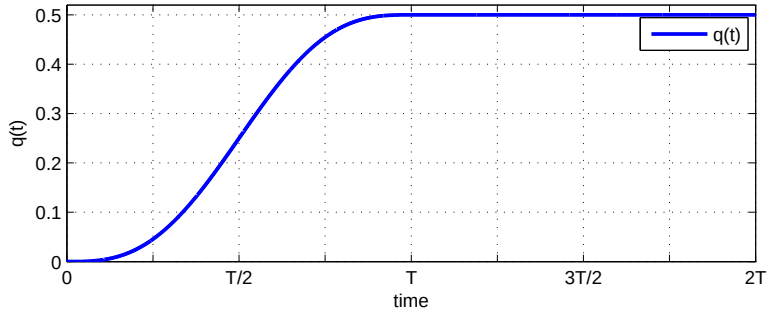

(b) Phase Smoothing Pulse

Figure 2.2: Full Response Raised Cosine Pulse (L = 1)

2.2.2.2 PARTIAL RESPONSE SYSTEMS

If the duration of the baseband shaping pulse $g(t)$ is longer than one symbol period, namely $L > 1$, then each data symbol affects the instantaneous frequency of the transmitted signal for more than one symbol interval. Thus, phase smoothing response $q(t)$ also reaches its final value $1/2$ after L symbol periods. This results in partial effects of each individual data to be seen both on its own and the next $L-1$ symbol intervals, hence the name *partial response* is given.

A partial response rectangular and a raised cosine baseband shaping pulses are given with the corresponding phase smoothing responses, with $L = 3$, in figures 2.3 and 2.4. The equation for the partial response rectangular pulse is,

$$g(t) = \begin{cases} \dfrac{1}{2LT} & 0 \le t \le LT \\ 0 & otherwise \end{cases} \tag{2.7}$$

and the equation for the partial response raised cosine pulse is,

$$g(t) = \begin{cases} \dfrac{1}{2LT}\left[1 - \cos\dfrac{2\pi t}{LT}\right] & 0 \le t \le LT \\ 0 & otherwise \end{cases} \tag{2.8}$$

Why do some systems need to use partial response signaling instead of using full response signaling which is simpler? The answer to this question lies in the spectral properties of the system. Using partial response CPM systems improves the spectral properties at almost all frequency band. As the length of the baseband shaping pulse increases, first sidelobes in the spectrum get considerably lower, and this improvement does not cause any increment in the probability of symbol error, [5].

Regardless of being full response or partial response, continuous phase modulation systems have memory inherently. In equation (2.4), it is obvious that the phase, $\phi(t, \overline{\alpha})$, of the transmitted signal depends on both the present and previous data. Using partial response signaling introduces additional memory to the system, originating from the previous symbols whose phase smoothing responses could not reach their final values of $1/2$ yet. So it can be con-

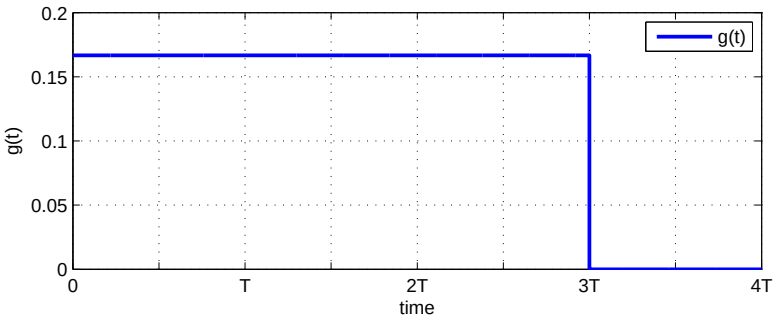

(a) Frequency Pulse

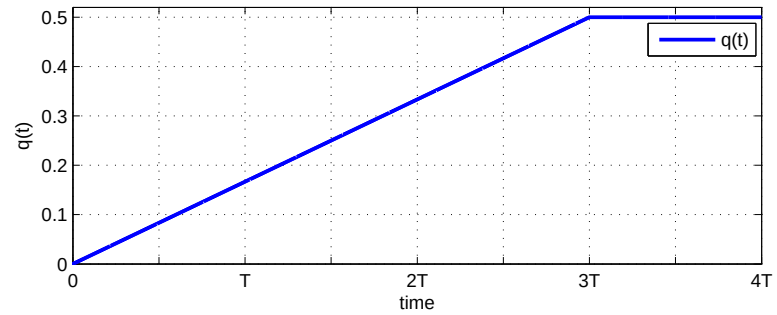

(b) Phase Smoothing Pulse

Figure 2.3: Partial Response Rectangular Pulse (L = 3)

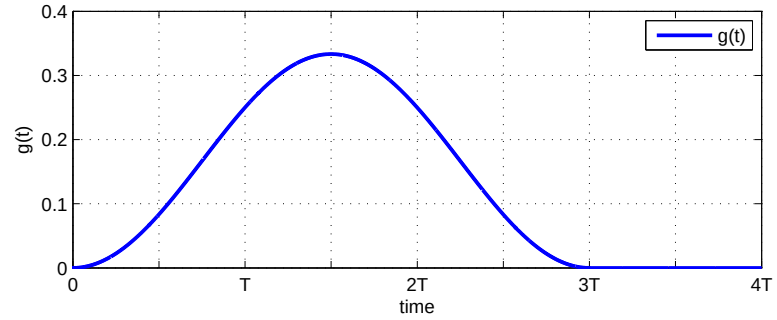

(a) Frequency Pulse

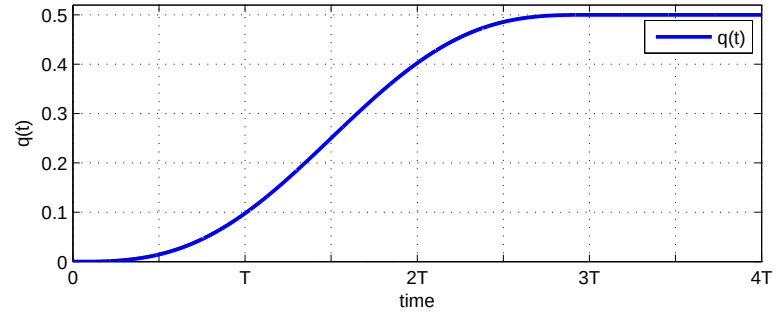

(b) Phase Smoothing Pulse

Figure 2.4: Partial Response Raised Cosine Pulse (L = 3)

cluded that the cost of spectral improvement gained by using partial response signaling is the additional memory introduced to the system, which increases the complexity of the receiver [2], [5].

2.3 LAURENT DECOMPOSITION

In 1986, a paper was published in *IEEE Transactions On Communications*, by Pierre A. Laurent, [7], explaining that any constant envelope binary phase modulation can also be expressed as the superposition of a finite number of *time-limited amplitude modulated pulses(AMP)*. This work includes only binary case with non-integer modulation index values. After the paper by Laurent, Mengali and Moore improved his work to the M-ary case in [8].

Before explaining the decomposition of CPM signals into amplitude modulated pulses, a revision of the signal model would be fine. It was shown in equation (2.1) that the transmitted CPM signal is represented as

$$s(t,\overline{\alpha}) = \sqrt{\frac{2E_s}{T}}\cos\left[2\pi f_c t + \phi(t,\overline{\alpha}) + \phi_0\right]$$

which can be written as

$$s(t,\overline{\alpha}) = \sqrt{\frac{2E_s}{T}}\mathbf{Re}\left[s_L(t,\overline{\alpha})\cdot e^{j2\pi f_c t}\right]$$

so the complex envelope, $s_L(t,\overline{\alpha})$, of a CPM signal with $\phi_0 = 0$ for binary coherent systems becomes,

$$s_L(t,\overline{\alpha}) = e^{j\phi(t,\overline{\alpha})} \tag{2.9}$$

In [7], [8], and [10], it has been shown that the baseband (complex envelope) CPM signal can be written as,

$$s_L(t,\overline{\alpha}) = \sum_{k=0}^{2^{L-1}-1}\sum_{n=0}^{N-1} b_{k,n}c_k(t-nT) \tag{2.10}$$

where the real pulses $c_k(t)$ are given as,

$$c_k(t) = u(t) \cdot \prod_{i=1}^{L-1} u(t + iT + \beta_{k,i} LT), \qquad 0 \leq k \leq 2^{L-1} - 1. \tag{2.11}$$

The function $u(t)$ in equation (2.11) is defined as,

$$u(t) = \begin{cases} \dfrac{\sin[2\pi h q(t)]}{\sin[\pi h]}, & 0 \leq t \leq LT, \\ u(2LT - t), & LT < t \leq 2LT, \\ 0, & otherwise \end{cases} \tag{2.12}$$

and $\beta_{k,i}$ in equation (2.11) are parameters taking on values 0 or 1. Actually, $\beta_{k,i}$ is the ith bit in the radix-2 representation of the value k, for any integer i in the interval $1 \leq i \leq 2^{L-1} - 1$. This can be modeled as,

$$k = \sum_{i=1}^{L-1} 2^{i-1} \beta_{k,i}, \qquad 0 \leq k \leq 2^{L-1} - 1.$$
$$\beta_{k,i} \in \{0, 1\} \tag{2.13}$$

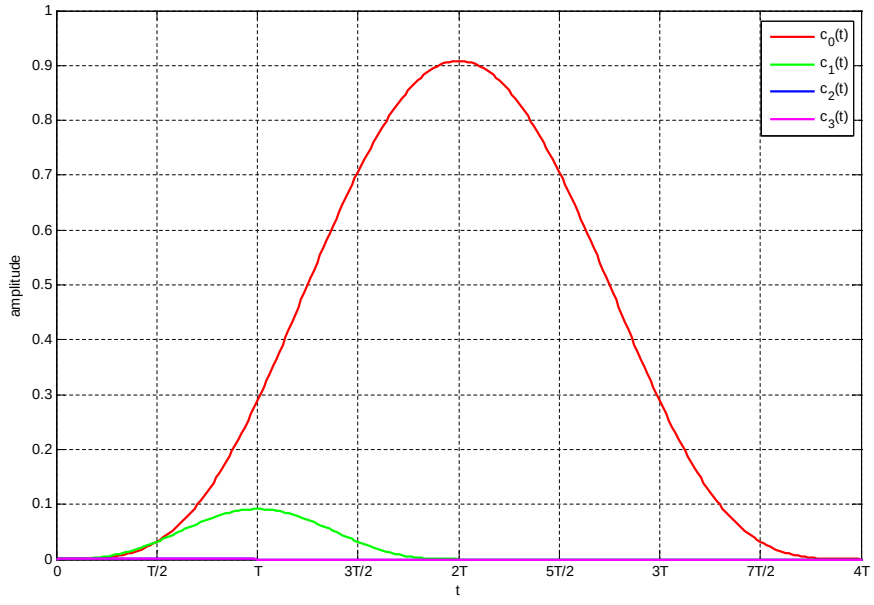

Figure 2.5: Laurent Pulses for Raised Cosine Pulse Shape with $L = 3$ and $h = 0.5$

Finally, the last parameter in equation (2.10) to be defined is the nonlinear coefficients $b_{k,n}$ which are related to the information data sequence $\overline{\alpha}$ by the relationship,

$$b_{k,n} = exp\Big\{ j\pi h\Big[\sum_{m=0}^{n} \alpha_m - \sum_{i=1}^{L-1} \alpha_{n-i}\beta_{k,i} \Big] \Big\} \tag{2.14}$$

Usage of Laurent Decomposition encourages complexity reduction in the receiver side. Because most of the energy of the transmitted signal is conveyed by the first few real Laurent pulses $c_k(t)$. In Figure 2.5, Laurent pulses for raised cosine pulse shape having a pulse length of $L = 3$, 3RC, with modulation index $h = 0.5$ is illustrated.

Hence, instead of using all the Laurent pulses at the receiver side, using the ones with high energy only, almost the same error performances with only a little degradation can be achieved. For example, in Figure 2.5, energy of the pulses $c_2(t)$ and $c_3(t)$ are almost negligible. So at the receiver side, using only two matched filters instead of four will probably result in the same error performance for this 3RC scheme. This is achieved by using $Q = L - 1 = 2$ instead of L in the equations given above for Laurent Decomposition.

CHAPTER 3

COHERENT CPM RECEIVER STRUCTURES

3.1 INTRODUCTION

In Chapter 2, it was mentioned that CPM is a constant envelope, nonlinear modulation scheme with attractive spectral properties that makes it so popular in digital communication area. These favorable properties of CPM makes it very *transmitter friendly*. Being constant envelope, leads to the usage of fully-saturated nonlinear amplifiers which are very much power efficient on the transmitter side, and also helps engineers to design simpler and cheaper transmitters. Choosing the right parameters for a CPM system brings the ability to control the power efficiency and the signal bandwidth to the designer, which makes this modulation technique very versatile and spectrum friendly.

Power efficiency, spectrum efficiency and being constant envelope are of course advantageous, but these characteristics are only related to the transmission part of the system. Of course, the transmitter side is not the only part of a communication system, there is also the receiver side. However, the receiver part of the communication system is not welcomed as well as the transmitter part by CPM. The nonlinear nature of CPM makes things more difficult at the receiver side; it becomes harder to demodulate the received signal and harder to synchronize. And spectrum efficiency is obtained by having longer and smoother baseband shaping pulses, which also increases the complexity of the receiver. As might be easily seen, the properties of continuous phase modulation leading to positive results at the transmitter side, somehow affects the receiver side negatively. This is a common trade-off that CPM system designers have to deal with.

In this chapter, optimum and suboptimum coherent receiver structures for CPM are reviewed. First the basic optimum maximum-likelihood receiver based on the phase trellis is discussed. It is followed by another optimum receiver structure based on the PAM signals obtained by the Laurent decomposition of CPM. The chapter ends with a brief discussion on reducing the state number to construct a suboptimum receiver from Laurent decomposition based receivers.

3.2 RECEIVERS BASED ON PHASE TRELLIS [2, 3]

Beginning with a brief review of some of the results obtained in the previous chapter and constructing the ideas about the receiver side on them will make the text more understandable. So, it is assumed that the baseband shaping pulse $g(t)$ has finite length LT and $g(t) = 0$ for $t < 0$ and $t > LT$. Since $g(t)$ is time limited, the phase smoothing response $q(t)$ is 0 for the negative values of t and has a constant value of $1/2$ for $t \geq LT$. Under these assumptions, the information carrying phase of a CPM signal can be rewritten as,

$$\begin{aligned} \phi(t,\overline{\alpha}) = &\quad 2\pi h \sum_{i=-\infty}^{n} \alpha_i q(t-iT) \\ = &\quad 2\pi h \sum_{i=n-L+1}^{n} \alpha_i q(t-iT) + \pi h \sum_{i=-\infty}^{n-L} \alpha_i, \\ &\qquad \textit{where } nT \leq t \leq (n+1)T. \end{aligned} \tag{3.1}$$

It is obvious from the equation (3.1) that the phase of the transmitted signal can be divided into two parts. One of them is the *cumulative phase*, defined as

$$\theta_n = \pi h \sum_{i=-\infty}^{n-L} \alpha_i \bmod 2\pi \tag{3.2}$$

The cumulative phase is constructed by past data symbols whose phase smoothing responses $q(t)$ have reached their final value of $1/2$ which is constant, and has no time-varying effect on the present symbol interval. Cumulative phase determines the number of phase states at the receiver side. The second phase component in equation (3.1) is the one related to the present symbol and the previous correlative symbols whose time-varying extensions caused by the phase smoothing responses can still be seen on the present symbol interval. This component is represented by,

$$\theta(t, \overline{\alpha_n}) = 2\pi h \sum_{i=n-L+1}^{n} \alpha_i q(t - iT) \tag{3.3}$$

Now we have the argument to define the phase of the transmitted signal by state representation. For any modulation index h and baseband shaping pulse $g(t)$, and for any symbol interval n (*where* $nT \leq t \leq (n+1)T$), $\phi(t, \overline{\alpha})$ is defined by the present symbol, α_n, the *correlative state vector*, $(\alpha_{n-1}, \alpha_{n-2}, \cdots, \alpha_{n-L+1})$, and the *phase state*, θ_n. Looking at the definition of the phase state in equation (3.2), it can be said that for irrational modulation indices, the state number is infinite. But for rational modulation indices $h = m/p$ (m, p relatively prime integers), there are p phase states for m even, and $2p$ phase states for m odd. The number of correlative phase states is finite and equals to M^{L-1}, which is simply 2^{L-1} for binary modulation schemes. Then the *total state* is defined by the L-tuple

$$\sigma_n = (\theta_n, \alpha_{n-1}, \alpha_{n-2}, \cdots, \alpha_{n-L+1}) \tag{3.4}$$

where the number of such states is,

$$\begin{aligned} S &= pM^{L-1} \qquad \text{for } m \text{ even in } h = m/p, \\ S &= 2pM^{L-1} \qquad \text{for } m \text{ odd in } h = m/p. \end{aligned} \tag{3.5}$$

Now after a brief review with the results obtained, the receiver side can be defined. In this thesis, we deal only with coherent receiver structures for AWGN channels. So the observed signal in the receiver is $r(t) = s(t, \tilde{\boldsymbol{\alpha}}) + n(t)$ where the noise $n(t)$ is Gaussian and white. The maximum-likelihood sequence estimation receiver maximizes the log likelihood function,

$$ln[p_{r(t)|\tilde{\boldsymbol{\alpha}}}(r(t) \mid \tilde{\boldsymbol{\alpha}})] \approx -\int_{-\infty}^{\infty} [r(t) - s(t, \tilde{\boldsymbol{\alpha}})]^2 dt \tag{3.6}$$

with respect to the *infinitely long estimated sequence* $\tilde{\boldsymbol{\alpha}}$ [2], [3]. Here $\tilde{\boldsymbol{\alpha}}$ is the maximum likelihood sequence estimate and $p_{r(t)|\tilde{\boldsymbol{\alpha}}}$ is the probability density function for the received signal $r(t)$ conditioned on the sequence $\tilde{\boldsymbol{\alpha}}$. Maximizing this function is theoretically equivalent to maximizing the correlation metric,

$$J(\tilde{\boldsymbol{\alpha}}) = \int_{-\infty}^{\infty} r(t) s(t, \tilde{\boldsymbol{\alpha}}) dt \tag{3.7}$$

But calculation of this metric is almost impossible because of the *infinitely long* sequence $\tilde{\boldsymbol{\alpha}}$. So, it can be defined for the nth symbol interval,

$$J_n(\tilde{\boldsymbol{\alpha}}) = \int_{-\infty}^{(n+1)T} r(t)s(t, \tilde{\boldsymbol{\alpha}})dt \tag{3.8}$$

which can be written in recursive form,

$$J_n(\tilde{\boldsymbol{\alpha}}) = J_{n-1}(\tilde{\boldsymbol{\alpha}}) + Z_n(\tilde{\boldsymbol{\alpha}}) \tag{3.9}$$

where the metric related to *only* the nth symbol interval is defined as,

$$Z_n(\tilde{\boldsymbol{\alpha}}) = \int_{nT}^{(n+1)T} r(t)\cos\left[\omega_0 t + \phi(t, \tilde{\boldsymbol{\alpha}}]\right)dt \tag{3.10}$$

As might be expected, the correlation metric $J(\tilde{\boldsymbol{\alpha}})$ is computed by using the recursive formulas in equations (3.9) and (3.10). The algorithm that maximizes the recursive log likelihood function up to the symbol interval n is called the *Viterbi algorithm*. This algorithm is run at the receiver to compute all the possible metrics for M^L possible sequences of $\tilde{\boldsymbol{\alpha}} = (\tilde{\alpha}_n, \tilde{\alpha}_{n-1}, \cdots, \tilde{\alpha}_{n-L+1})$ and p or $2p$ possible phase states $\tilde{\theta_n}$. So the receiver computes a total of pM^L values of Z_n for m even or $2pM^L$ values of Z_n for m odd, where $h = m/p$. For complex baseband domain, Z_n in equation (3.10) can be written as,

$$Z_n(\tilde{\boldsymbol{\alpha}}_{\boldsymbol{n}}, \tilde{\theta_n}) = \mathbf{Re}\left\{ \int_{nT}^{(n+1)T} r(t)e^{-j[\theta(t,\tilde{\boldsymbol{\alpha}}_{\boldsymbol{n}})+\tilde{\theta_n}]}dt \right\} \tag{3.11}$$

It can easily be seen that the partial metric $Z_n(\tilde{\boldsymbol{\alpha}}_{\boldsymbol{n}}, \tilde{\theta_n})$ is computed by sampling the output of a complex matched filter at $t = (n+1)T$ fed by the received signal $r(t)$ and taking the real part of the output. And for computation of all the possible sequences $(\tilde{\boldsymbol{\alpha}}_{\boldsymbol{n}}, \tilde{\theta_n})$, a bank of matched filters is needed. Then the optimum receiver can be implemented as in Figure 3.1. The number of matched filters, K, is equal to the number of all possible transmitted signals, which is pM^L or $2pM^L$ for m even and odd, respectively, where $h = m/p$.

To implement a more practical receiver having real matched filters, equation (3.11) can be written as,

$$
\begin{aligned}
Z_n(\tilde{\boldsymbol{\alpha}}_{\boldsymbol{n}}, \tilde{\theta}_n) \;=\; & cos(\tilde{\theta}_n) \int_{nT}^{(n+1)T} \hat{I}(t) \cos\left[\theta(t, \tilde{\boldsymbol{\alpha}}_{\boldsymbol{n}})\right] dt \\
& + cos(\tilde{\theta}_n) \int_{nT}^{(n+1)T} \hat{Q}(t) \sin\left[\theta(t, \tilde{\boldsymbol{\alpha}}_{\boldsymbol{n}})\right] dt \\
& + sin(\tilde{\theta}_n) \int_{nT}^{(n+1)T} \hat{Q}(t) \cos\left[\theta(t, \tilde{\boldsymbol{\alpha}}_{\boldsymbol{n}})\right] dt \\
& - sin(\tilde{\theta}_n) \int_{nT}^{(n+1)T} \hat{I}(t) \sin\left[\theta(t, \tilde{\boldsymbol{\alpha}}_{\boldsymbol{n}})\right] dt
\end{aligned}
\tag{3.12}
$$

where $\hat{I}(t)$ and $\hat{Q}(t)$ are in-phase and quadrature components of the received signal $r(t)$, respectively. In this case there are $4M^L$ matched filters in the receiver [2].

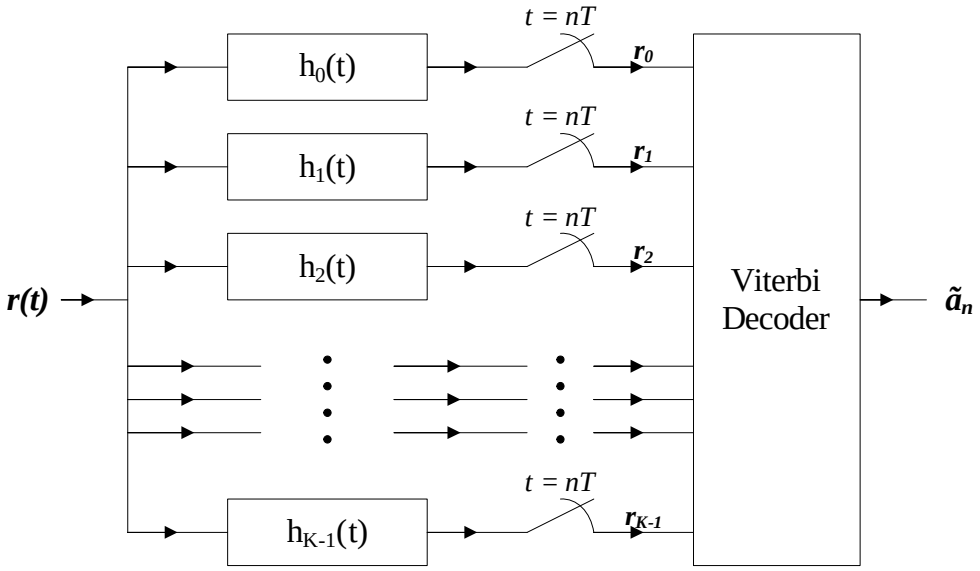

Figure 3.1: Optimum MLSE Viterbi receiver with complex matched filters

3.3 RECEIVERS BASED ON LAURENT DECOMPOSITION [10, 11]

The observed signal in the receiver to be processed is

$$
r(t) = s(t, \boldsymbol{\alpha}) + n(t) \tag{3.13}
$$

where $s(t, \boldsymbol{\alpha})$ is the transmitted complex baseband signal, and $n(t)$ is complex-valued additive

white Gaussian noise with one-sided power spectral density of N_0. The optimum receiver that minimizes the symbol error probability is the one that maximizes the correlation metric,

$$\mathbf{Re}\left\{\int_{-\infty}^{\infty} r(t)s^*(t,\boldsymbol{\alpha})dt\right\} \tag{3.14}$$

because all the possible transmitted signals have the same energy and the same a priori probabilities. Since the transmitted signal $s(t,\boldsymbol{\alpha})$ has been defined in equation (2.10) as,

$$s(t,\boldsymbol{\alpha}) = \sum_{k=0}^{2^{L-1}-1}\sum_{n=0}^{N-1} b_{k,n}c_k(t-nT) \tag{3.15}$$

the metric to be calculated at the receiver can be redefined as,

$$\mathbf{Re}\left\{\int r(t)s^*(t,\boldsymbol{\alpha})dt\right\} = \mathbf{Re}\left\{\sum_{n}\sum_{k=0}^{2^{L-1}-1} b_{k,n}^* \int_{-\infty}^{\infty} r(t)c_k(t-nT)dt\right\} \tag{3.16}$$

Now, if the argument of the integral operator in equation (3.16) is defined as,

$$r_{k,n} = \int_{-\infty}^{\infty} r(t)c_k(t-nT)dt = r(t)\otimes c_k(-t)|_{t=nT} \tag{3.17}$$

then the partial metric that the receiver must calculate is given by,

$$\lambda_n = \mathbf{Re}\left\{\sum_{k=0}^{2^{L-1}-1} r_{k,n}b_{k,n}^*\right\} \tag{3.18}$$

Finally, equation (3.16) can be reexpressed as,

$$\mathbf{Re}\left\{\int r(t)s^*(t,\boldsymbol{\alpha})dt\right\} = \sum_{n}\lambda_n \tag{3.19}$$

The receiver based on Laurent Decomposition can be implemented as in Figure 3.2. In this case, the number of matched filters, K, is equal to the number of Laurent pulses, $c_k(t)$, hence $K = 2^{L-1}$. Sampled outputs of the matched filters are preprocessed in *Branch Metric Computer* block to generate the metrics needed to feed the Viterbi decoder. These metrics, λ_n, represent all possibilities for the transmitted signal. So the number of the computed branch

metrics is $S = pM^L$ or $S = 2pM^L$ for m even and odd, respectively, where $h = m/p$. It is the same as in the optimum CPM receiver based on phase trellis.

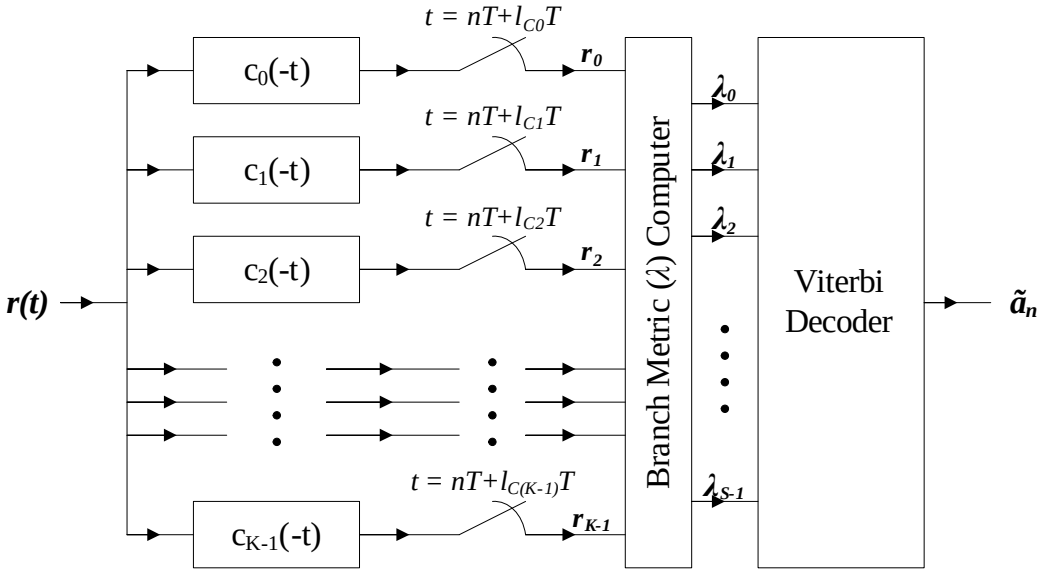

Figure 3.2: LD Based Receiver with real matched filters

The usage of LD based receivers provides a complexity reduction even in the optimal case, where all the Laurent pulses are employed in the filter bank. Further reduction in complexity of the receiver can be achieved by omitting the Laurent pulses having negligible energy, as described in Section 2.3. That is the key point used in this study to reduce receiver complexity.

CHAPTER 4

SPECTRALLY EFFICIENT PULSE SHAPES FOR CPM SIGNALS

4.1 INTRODUCTION

In July 2001, an M.S. thesis, titled *"New Pulse Shapes For CPM Signals"* [5], was conducted to the literature by Ç. Enis Doyuran. The objective of the thesis is to find new pulse shapes for CPM signals which have better spectral and detection performance than the spectrally efficient GMSK signal currently used in the GSM modulation scheme. Unlike the older methods which used the *RMS bandwidth* or *effective bandwidth* to represent spectral occupancy, in this thesis, the *GSM spectral standards* were used for determining the spectral criterion, because the RMS bandwidth approach can not control the sidelobes and the spectrum near carrier frequency.

For comparison of detection performance of the new pulse shapes, the criterion was the error probability. Minimum Euclidean distance between any two of the signals present in the signal space was used to calculate the error probability for an optimum detector at large SNR. Then, to minimize the error probability, a maximization procedure was held for the minimum Euclidean distance.

As a summary, there are two criteria for comparison of the new pulse shapes with the existing pulse shapes used currently in the GSM modulation scheme. First one is that the new pulse shapes have to give higher values for the minimum Euclidean distance than the existing ones; and the second one is that the power spectra of the new pulse shapes must stay within the

spectral standards of GSM (see Figure 4.1). As might be expected, to realize the aim, a vast amount of power spectrum density (PSD) and minimum Euclidean distance computations are required. Hence, efficient calculation methods derived by T. Aulin and Carl-Erik W. Sundberg were preferred in the thesis, considering the computational complexity.

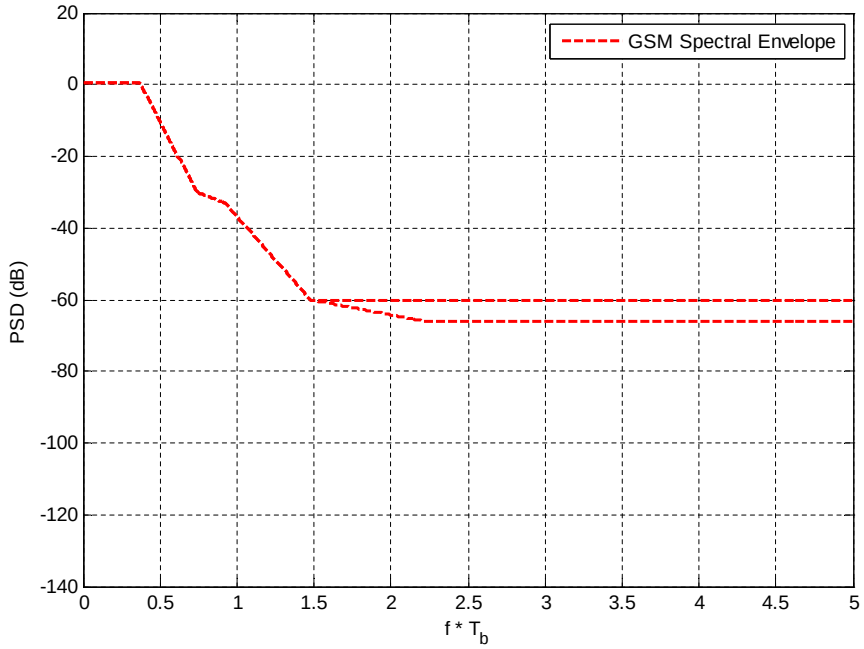

Figure 4.1: GSM Spectral Envelope as defined in [6],[20]

In this chapter, first the methods for PSD and minimum Euclidean distance calculations used in Ç. Enis Doyuran's thesis are briefly explained. Then some information about how the pulse shaping is done by using the exact and polynomials and polynomials with free parameters is given. Lastly, the new optimum pulse shapes found throughout the study are given.

4.2 POWER SPECTRUM AND MINIMUM EUCLIDEAN DISTANCE

4.2.1 CALCULATION OF POWER SPECTRUM

A quite versatile and straightforward numerical method is used in calculation of the power spectral density of CPM signals. In the method chosen, any baseband pulse shape (frequency

pulse) with an arbitrary modulation index can be used. The distribution of the independent data symbols can also be arbitrary, having any probability density function. As mentioned previously, the method is straightforward. First the *baseband autocorrelation function* of the desired CPM signal is calculated, and then it is followed by the computation of the power spectrum by numerically Fourier transforming the previously calculated autocorrelation function.

Using the complex notation, the transmitted signal in equation (2.1) can be written as,

$$s(t,\overline{\alpha}) = \sqrt{2P}\mathbf{Re}\left[e^{j\phi(t,\overline{\alpha})}e^{j2\pi f_c t}\right] \tag{4.1}$$

where P is the constant transmitted power that is equal to E_s/T. Then the autocorrelation function can be defined as,

$$r(\tau) = \langle E\{s(t+\tau,\overline{\alpha})s(t,\overline{\alpha})\}\rangle \tag{4.2}$$

where $\langle\cdot\rangle$ is the time-averaging operator, $E\{\cdot\}$ is the expectation operator with respect to the random variable $\overline{\alpha}$. If the CPM signal defined in equation (4.1) is inserted into equation (4.2),

$$r(\tau) = P\mathbf{Re}\{R(\tau)e^{j2\pi f_c\tau}\} \tag{4.3}$$

where

$$R(\tau) = \langle E\{e^{j\phi(t+\tau,\overline{\alpha})}e^{-j\phi(t,\overline{\alpha})}\}\rangle \tag{4.4}$$

is called the *complex baseband autocorrelation function*. Now applying the rest of the numerical PSD calculation method is easy. First, calculate the complex baseband autocorrelation function, and then numerically Fourier transform it to obtain the PSD. Under the light of references [5] and [15], the complex baseband autocorrelation function $R(\tau)$ can be calculated as,

$$
\begin{aligned}
R(\tau) &= R(\tau' + mT) \\
&= \frac{1}{T}\int_0^T \prod_{i=1-L}^{m+1} \left\{ \sum_{\substack{k=-(M-1) \\ k\ odd}}^{M-1} p_k \exp\left(j2\pi hk[q(t+\tau'-(i-m)T) - q(t-iT)]\right) \right\} dt \\
&\quad \tau = \tau' + mT, \qquad 0 \le \tau' \le T, \qquad m = 0, 1, 2, \ldots
\end{aligned}
\tag{4.5}
$$

over the interval $\tau \in [0, (L+1)T]$. And the power spectrum is defined as [5], [15],

$$
S(f) = 2\mathbf{Re}\left\{ \int_0^{LT} R(\tau) e^{-j2\pi f\tau} d\tau + \frac{e^{-j2\pi fLT}}{1 - C_\alpha e^{-j2\pi fT}} \int_0^T R(\tau + LT) e^{-j2\pi f\tau} d\tau \right\} \tag{4.6}
$$

where

$$
C_\alpha = \sum_{\substack{k=-(M-1) \\ k\ odd}}^{M-1} p_k e^{j\pi hk} \tag{4.7}
$$

In the case of uniform probability density function assumption for the identically distributed statistically independent data symbols, the a priori probabilities p_k in equations (4.5) and (4.7) can be taken as,

$$
p_k = P\{\alpha_i = k\} = 1/M, \qquad k = \pm 1, \pm 3, \cdots, \pm(M-1), \quad i = 0, \pm 1, \pm 2, \ldots
$$

By using the method and the equations given above, one can calculate the power spectral density of a desired CPM signal with any baseband shaping pulse $g(t)$, any modulation index h, and any data symbol probability density function.

4.2.2 CALCULATION OF MINIMUM EUCLIDEAN DISTANCE

Detection of transmitted data symbols as reliably as possible is one of the main purposes of digital communication systems. The criterion to measure this quality is the symbol error probability. In AWGN channels, for large signal to noise ratios, the probability of error at the receiver end is found as,

$$
P_e \approx K_{d_{min}} \cdot Q\left(\left(d^2_{min} \frac{E_b}{N_o} \right)^{1/2} \right) \tag{4.8}
$$

where $K_{d_{min}}$ is the average number of paths that give the minimum distance, d^2_{min} is the normalized minimum Euclidean distance, E_b is the bit energy, N_o is the one-sided power spectral density, and

$$Q(x) = \frac{1}{\sqrt{2\pi}} \int_x^\infty e^{-\frac{t^2}{2}} dt \tag{4.9}$$

is the so-called *Q-function* that provides a compact formulation of the probability of bit error, [21]. Looking at the equation (4.8), it is obvious that the probability of erroneous detection is inversely proportional to the normalized minimum Euclidean distance d^2_{min}. So, it can be said that the survey about reliable communication systems is a simplified problem of finding better d^2_{min}'s.

In the thesis by Ç. E. Doyuran, the method to calculate the normalized minimum Euclidean distance starts with the calculation of an upper bound d^2_B. The idea is that d^2_{min} is the same as d^2_B as long as the observation time of the signal is long enough. As indicated in the references [1], [2] and [5], the upper bound on the normalized minimum Euclidean distance as a function of the modulation index, h, size of the data alphabet, M, and the phase smoothing response, $q(t)$ is defined as,

$$d^2_B(h) = \log_2(M) \cdot \min_{1 \le k \le M-1} \left\{ (L+1) - \frac{1}{T} \int_0^{(L+1)T} \cos\Big[2\pi h \cdot 2k(q(t) - q(t-T)) \Big] dt \right\} \tag{4.10}$$

Now the upper bound can be calculated for a CPM signal with known parameters. The problem is to find the minimum Euclidean distance more efficiently with the help of this bound. The normalized squared Euclidean distance is given by [5],

$$d^2(\overline{\gamma}_N, h) = \log_2(M) \left(N - \frac{1}{T} \int_0^{NT} \cos\left[\phi(t, \overline{\gamma}_N)\right] dt \right) \tag{4.11}$$

where $\overline{\gamma}_N$ is the difference sequence and $\phi(t, \overline{\gamma}_N)$ is the phase difference trajectories defined by [2],

$$\phi(t, \overline{\gamma}_N) = 2\pi h \sum_{i=-\infty}^{\infty} \gamma_i q(t - iT), \quad \gamma_i = 0, \pm 2, \pm 4, \cdots, \pm 2(M-1). \tag{4.12}$$

Using equations (4.11) and (4.12), the normalized minimum Euclidean distance can be found by an efficient algorithm searching the minimum of the squared Euclidean distances, namely,

$$d^2_{min,N}(h) = \min_{\overline{\gamma}_N}\{d^2(\overline{\gamma}_N, h)\} \tag{4.13}$$

where $\overline{\gamma}_N$ is defined as,

$$\begin{aligned} &\gamma_i = 0, && i < 0 \\ &\gamma_0 = 0, 2, 4, 6, \cdots, 2(M-1), && \\ &\gamma_i = 0, \pm 2, \pm 4, \cdots, \pm 2(M-1), && i = 1, 2, \cdots, N-1. \end{aligned} \tag{4.14}$$

Unlike the conventional brute-force algorithms which grow exponentially with N, a fast algorithm that increases linearly with N was used to calculate d^2_{min} in Doyuran's work. The algorithm uses the recursive equation below to find the minimum distance, and the upper bound d^2_B is used to truncate the search trees by eliminating the squared distances which are greater than d^2_B. This recursive equation is

$$d^2(\overline{\gamma}_{N+1}, h) = d^2(\overline{\gamma}_N, h) + \log_2(M)\left(1 - \frac{1}{T}\int_{NT}^{NT+1} \cos\left[\phi(t, \overline{\gamma}_{N+1})\right]dt\right). \tag{4.15}$$

4.3 POLYNOMIAL APPROACH FOR PULSE SHAPING

Finding *optimum* pulse shapes for CPM signals better than the ones used in GSM was the main goal of the thesis conducted by Doyuran. To realize this goal, an optimization problem for $g(t)$, the baseband shaping pulse, was performed aiming to find the highest minimum Euclidean distance to have better error probabilities, in conjunction with the constraint that the power spectrum density of the found pulse shapes must stay below the GSM spectral envelope existing in the standards. This optimization problem was conducted using the derivations explained in the previous sections of the chapter.

The first approach Ç. E. Doyuran tried was using sum of raised cosine pulses with duration of one symbol interval. It was discovered that to provide the PSD to stay within the GSM

constraints, low values of modulation indices had to be used. But using low values of modulation index results in low values of the minimum Euclidean distance, in other words poor error performance. Then another approach, using polynomials to represent pulse shapes, was used. Because, by using sufficiently high degree polynomials, any smooth pulse shape can be approximated, having better power spectrum[5].

To obtain pulse shapes by using polynomials, some constraints on the baseband shaping pulse have to be used. One of these constraints is the normalization constraint that the integral of $g(t)$ has to be $1/2$. Other constraints imposed on $g(t)$ are [5]:

- $g(t) = 0$ when $t = 0$ and $t = LT$,
- the first derivative $g'(t) = 0$ when $t = 0$ and $t = LT$,
- the second derivative $g''(t) = 0$ when $t = 0$ and $t = LT$,
- the third derivative ... and so on.

As more constraints are used in finding a suitable polynomial, higher degree polynomials have to be handled to satisfy them. In Doyuran's work, two optimum pulse shapes were found having better error performances under the constraint of staying below the spectral limits of GSM. These pulse shapes are illustrated in figures 4.2 and 4.3. The first one is a pulse shape with duration of three symbol intervals ($L = 3$), and the second one is a pulse shape with seven symbol interval length ($L = 7$).

The pulse shape in Figure 4.2 is obtained by using $8^{\text{th.}}$ degree polynomials with 4 *free parameters*, meaning that only 5 constraints are used for 9 parameters required to represent an $8^{\text{th.}}$ degree polynomial, in optimization. The other pulse shape in Figure 4.3 is obtained by using $8^{\text{th.}}$ degree *exact* polynomials, which means 9 constraints are used for 9 equations existing in the optimization problem.

These pulse shapes are the ones that this thesis aims to design affordable receivers which are practically easy to implement. The pulse shape with $L = 3$ has an error performance 1.08 dB better than the standard GMSK signal used in the GSM modulation scheme ($BT = 0.3$,

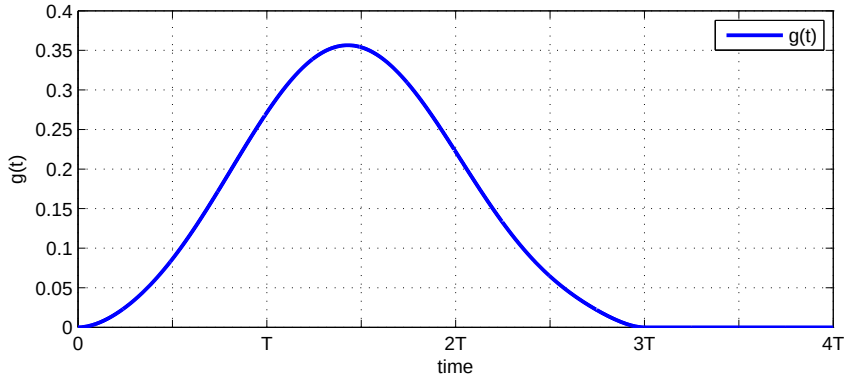

Figure 4.2: Optimum pulse shape with $L = 3$

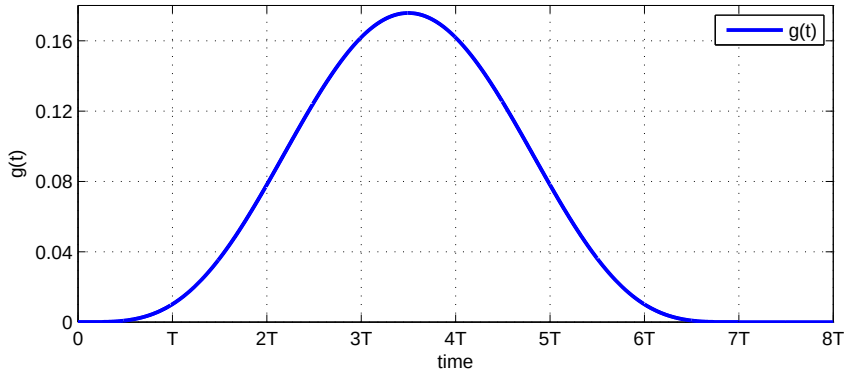

Figure 4.3: Optimum pulse shape with $L = 7$

$h = 0.5$), when used with a modulation index of $h = 0.5870$. The pulse shape with duration $L = 7$ is much better. When used with a modulation index $h = 0.8633$, it is 2.30 dB better than the mentioned GMSK signal.

CHAPTER 5

PROPOSED RECEIVERS AND SIMULATION RESULTS

5.1 INTRODUCTION

In the previous chapters, after giving some basic information about continuous phase modulation, the main receiver structures for that modulation type are given and a class of new pulse shapes found in a recent study are mentioned. Now in this chapter, proposed receivers will be introduced for those new pulse shapes. First the simulation models used in MATLAB software to realize these receivers are given, with an example of verification of the model by the use of the well-known MSK signal. Then the optimum receiver for the GMSK signal used in GSM ($BT = 0.3$, $h = 0.5$ & $L_t = 7$) is considered for comparison with the proposed receivers to see the performance gained with the new pulse shapes. Lastly, the proposed receivers for the new pulse shapes will be introduced, both for $L = 3$ and $L = 7$ cases as described in the original work of Mr. Doyuran.

5.2 SIMULATION MODELS

Assuring the accuracy of a design necessitates a test set-up to verify the work done and also to measure the performance of the built structure. In this case, the test set-up is a communication system which consists of a transmitter, a channel and the receiver to be tested. A simple communication system is illustrated in Figure 5.1. Here, the transmitter is a CPM baseband modulator, the channel is an AWGN channel and the receiver is the structure to measure the performance of.

The most common method to measure the performance of a digital receiver is to obtain its bit

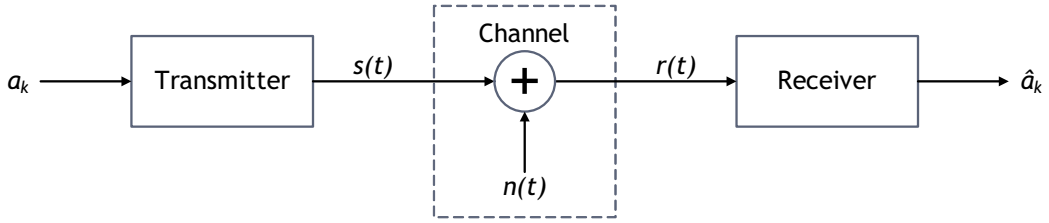

Figure 5.1: Main blocks of the simulation model: the transmitter, AWGN channel and the receiver

error rate (BER) characteristics. To reach this goal using the methods of computer simulation, the first thing to do is generating a pseudo-random bit sequence and saving it with a name like "*transmitted bits*". Then this bit sequence is fed into the transmitter and the transmitted baseband signal is obtained at the output. After passing the transmitted signal through the channel, the received signal is obtained that is to be fed into the receiver. The received signal is disturbed with noise (and distorted by the channel response if it exists). Feeding the received signal to the receiver gives a "*received bits*" at the output. And finally, the output bit sequence of the system, the received bits, is compared with the input bit sequence that was saved before, the transmitted bits, and the number of bits in error is counted. The number of bit errors divided by the length of the whole bit sequence gives the so-called simulated bit error rate. This procedure is carried on with changing the noise power at every step, which is added within the channel. In the end, a graph of bit error rate with respect to signal to noise ratio is obtained, and that is the receiver performance obtained by simulation. While dealing with computer simulation studies, a very important point to keep in mind is statistical validity. An adequate number of errors must have been generated in each run to be statistically significant. For example, in a simulation run for an SNR value where approximately 10^{-5} bit errors are expected, there will most likely be no errors seen if the simulation is conducted with 1000 bits. However, this does not mean that the bit error rate for this SNR value is zero, it means that we did not use an adequate number of bits in our transmitted signal to see an error. In order to reach statistical confidence, a minimum of 100 errors have been generated for each SNR value in every simulation conducted in this study. This is mostly realized by taking the mean of the results of similar simulations in which the sum of errors exceed 100.

In the simulations conducted throughout the study, it is always dealt with baseband signals. So, the signal generated by the transmitter is a complex-valued signal which is disturbed by a

complex-valued noise at the channel. Hence the receiver is also designed to receive baseband signals only; no passband to baseband down conversion or low-pass filtering is included. Under these circumstances, the main blocks of the simulation model are introduced in detail in the following sections.

5.2.1 TRANSMITTER

In a digital communication system, transmitter is the block where the signal to be transmitted is generated from a sequence of information carrying data symbols, which are data bits in this binary case. Therefore the purpose of our transmitter block is to generate a signal from a random bit sequence.

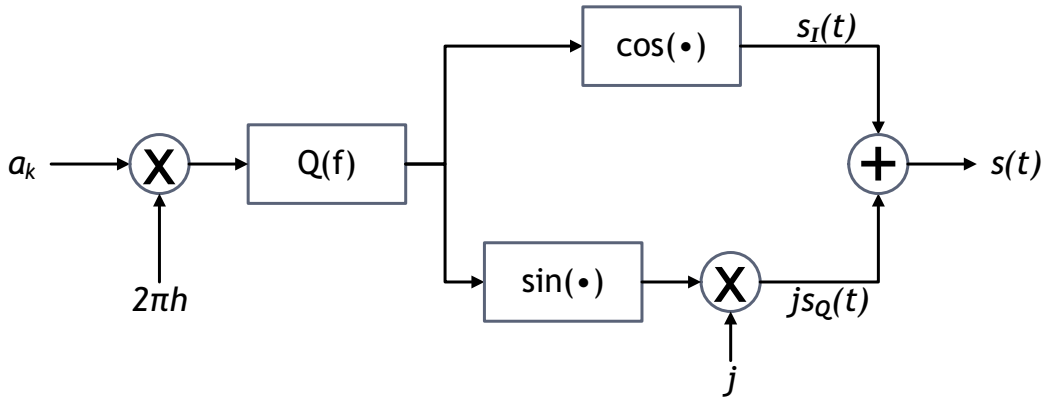

Figure 5.2: Baseband transmitter structure used in BER simulations

As mentioned before, the transmitter block described herein is a baseband continuous phase modulator, producing a complex-valued signal. In previous chapters it was shown that,

$$s(t,\overline{\alpha}) = \sqrt{\frac{2E}{T}}\cos\left[2\pi f_c t + \phi(t,\overline{\alpha})\right] \tag{5.1}$$

is the transmitted signal representation for CPM. In the case where unit energy ($E = 1$) and unit symbol period ($T = 1$) is assumed, the E and T parameters can be omitted from the equation, leading into a simpler representation. Hence, throughout the simulation unit energy transmitted signals having symbol period of 1 (the unit of the period (*ns, us, etc.*) is not relevant for the simulation case) is assumed. Regarding this assumption, the signal format

for the transmitter becomes,

$$\begin{aligned} s(t,\overline{\alpha}) &= \sqrt{2}\mathbf{Re}\left\{s_L(t,\overline{\alpha})e^{j2\pi f_c t}\right\} \\ s_L(t,\overline{\alpha}) &= e^{j\phi(t,\overline{\alpha})} \\ &= \cos\left[\phi(t,\overline{\alpha})\right] + j\sin\left[\phi(t,\overline{\alpha})\right] \end{aligned} \tag{5.2}$$

The transmitter block diagram used in simulations is illustrated in Figure 5.2. The input of the system is the random data bit sequence formed with $\overline{\alpha_k}$, which are the elements of the set $\{-1, 1\}$. To constitute this data sequence, first a pseudo-random bit sequence $\overline{d_k}$ of $\{0, 1\}$ is generated, and then transformed into $\overline{\alpha_k}$ by the following equation,

$$\alpha_k = 2 \cdot d_k - 1 \tag{5.3}$$

After this transformation, every data bit in the sequence is multiplied with $2\pi h$, where h is the modulation index which is a constant parameter for the transmitter block, because only single modulation index CPM schemes are governed by this study. This multiplication with a constant is followed by a pulse-shaping filter block whose overall impulse response is the same as the phase smoothing response, $q(t)$, of the selected modulation scheme. This filter is actually formed by two sub-components; first one is the pulse-shaping filter with the impulse response of the baseband shaping pulse, $g(t)$, whose length equals to LT, and second one is an integrator to yield in the shape of phase smoothing response, $q(t)$. After this filter block, the information-carrying phase is obtained as in equation (5.4). The important thing to keep in mind here is that the data bits are taken into the transmitter successively with the symbol period T, but the pulse-shaping filter has a length that is equal to LT.

$$\phi(t,\overline{\alpha_k}) = 2\pi h \sum_{k=0}^{\infty} \alpha_k q(\tau - kT) \tag{5.4}$$

Following the formation of the information-carrying phase there are two branches in Figure 5.2. These branches calculate the real and the imaginary parts of the complex transmitted signal. At the upper branch, the cosine of the calculated phase signal is computed, which results in the in-phase component of the transmitted signal. However, at the lower branch, the sine of the information bearing phase is computed and multiplied by "j" to yield the imaginary quadrature component.

$$\begin{aligned} s(t) &= s_I(t) + j s_Q(t) \\ &= \cos\left[\phi(t, \overline{\alpha})\right] + j \sin\left[\phi(t, \overline{\alpha})\right] \end{aligned} \tag{5.5}$$

Finally, these two components, in-phase and quadrature, are added to yield the complex base-band transmitted signal at the output of the transmitter.

5.2.2 AWGN CHANNEL

The transmitted signal formed by the CPM baseband transmitter block passes through a channel. The channel is simulated by simply adding a controlled amount of noise to the transmitted signal. The noise added to the signal is additive white noise having a Gaussian distribution (AWGN), hence the channel is called *AWGN channel*. This noisy signal then becomes the input to the receiver block.

The goal of the simulations conducted throughout this study is to obtain the BER performance of the receiver. Bit error rate performance is usually plotted on a two-dimensional graph. The *x-axis* of this graph is the normalized signal to noise ratio (SNR), which is expressed as E_b/N_0 in decibels (dB) generally, where E_b is the received bit energy and N_0 is the one-sided power spectral density of the noise. The *y-axis* of the curve is the dimensionless bit error rate, usually expressed in logarithmic scale, values indicated by powers of ten.

Simulations aiming to yield BER graphs, have to result in a series of calculated points with different E_b/N_o values used in each run. Therefore, at every step of the simulations an additive white Gaussian noise having a different power spectral density has to be computed. For that controlled amount of noise added at each step, the following procedure is used

Since the purpose of BER graph plot necessitates the establishment of the E_b/N_0 values in decibels (dB), the first job to do is to find the one-sided power spectral density value, N_0, that yields the desired E_b/N_0 value with the predefined bit energy value of $E_b = 1$. Hence, using the relation,

$$N_0 = E_b \cdot 10^{\left(\frac{-(E_b/N_0)_{(dB)}}{10}\right)} \tag{5.6}$$

gives that N_0 value. Since the one-sided power spectral density of the noise determines how much noise power is present in a 1.0 Hz bandwidth of the signal, the signal bandwidth must be known to find the total amount of noise power that affects the transmitted signal. In computer simulations, all the signals are represented as discrete-time signals as they were sampled with a sampling rate of f_s. The sampling rate f_s determines how many samples are to be used to represent one symbol period of the original signal. Regarding the sampling theorem, the bandwidth of a sampled signal, that has a sampling rate of f_s, is at most half the sampling rate. Thus, the noise power affecting the transmitted signal is,

$$\begin{aligned} P_{noise} &= N_0 \cdot B_{noise} \\ &= \frac{N_0 \cdot f_s}{2} \end{aligned} \tag{5.7}$$

Since the AWGN has zero mean, the noise power, P_{noise}, equals to the noise variance, σ_n. Now that all the information regarding to the noise is known already, the only thing to do is to produce a noise sequence having a variance of σ_n. For this process to realize, two zero-mean Gaussian distributed random signals with durations equal to the length of the transmitted signal with unit variance is generated in MATLAB software, $n_{I_{\sigma=1}}(t)$ and $n_{Q_{\sigma=1}}(t)$. Then these unity variance noise signals are transformed into one complex noise with variance σ_n by the following equation.

$$n(t) = \sqrt{\sigma_n} \cdot \left[n_{I_{\sigma=1}}(t) + j n_{Q_{\sigma=1}}(t)\right] \tag{5.8}$$

The transmitted signal plus the additive white Gaussian noise defined above together form the *received signal* that is the input for the receiver.

5.2.3 THE RECEIVER

The last block of the simulation model is the receiver, where the noisy signal corrupted by additive white Gaussian noise at the channel is demodulated and decoded to give the data

bits sent by the transmitter. As mentioned before, only coherent receivers that have perfect synchronization with symbol timing are governed by this thesis study.

In Chapter 3, it was noted that CPM receivers are a type of maximum likelihood sequence estimating (MLSE) receivers which maximizes the log-likelihood function,

$$ln[p_{r(t)|\tilde{\boldsymbol{\alpha}}}(r(t) \mid \tilde{\boldsymbol{\alpha}})] \approx -\int_{-\infty}^{\infty} [r(t) - s(t, \tilde{\boldsymbol{\alpha}})]^2 dt \tag{5.9}$$

with respect to the *infinitely long estimated sequence* $\tilde{\boldsymbol{\alpha}}$; $\tilde{\boldsymbol{\alpha}}$ is the maximum likelihood sequence estimate and $p_{r(t)|\tilde{\alpha}}$ is the probability density function for the received signal $r(t)$ conditioned on the sequence $\tilde{\boldsymbol{\alpha}}$. Maximizing this log-likelihood function up to the nth symbol interval theoretically corresponds to maximizing the correlation metric,

$$J_n(\tilde{\boldsymbol{\alpha}}) = \int_{-\infty}^{(n+1)T} r(t)s(t, \tilde{\boldsymbol{\alpha}})dt \tag{5.10}$$

which can be defined in the following recursive form leading to *Viterbi decoder* usage,

$$J_n(\tilde{\boldsymbol{\alpha}}) = J_{n-1}(\tilde{\boldsymbol{\alpha}}) + Z_n(\tilde{\boldsymbol{\alpha}}) \tag{5.11}$$

where $Z_n(\tilde{\boldsymbol{\alpha}})$ is the *branch metric* that is *only* related to the nth symbol interval.

There are two types of receiver structures used in simulations as stated before. These are the *Optimum CPM Receiver* and *LD (Laurent Decomposition) Based Receiver*. Both of these receiver structures have a *matched-filter bank* at first step and a *Viterbi decoder* at the end. They only differ in the filter bank structure, and the LD based receiver has an additional *branch metric computer* block just before the Viterbi decoder section.

5.2.3.1 OPTIMUM CPM RECEIVER

A receiver based on the trellis structure that consists of a bank of filters, which are matched to each branch in the phase trellis, followed by a maximum likelihood sequence estimating

(MLSE) decoder is the optimum receiver for continuous phase modulation [2]. Since MLSE decoder runs on an infinitely long sequence theoretically, this is achieved by a decoder that uses the well-known Viterbi algorithm, namely *Viterbi decoder* or *Viterbi processor*. Viterbi algorithm runs on a finite sequence recursively, as in equation (5.11), to yield maximum likelihood sequence estimation on a long time period.

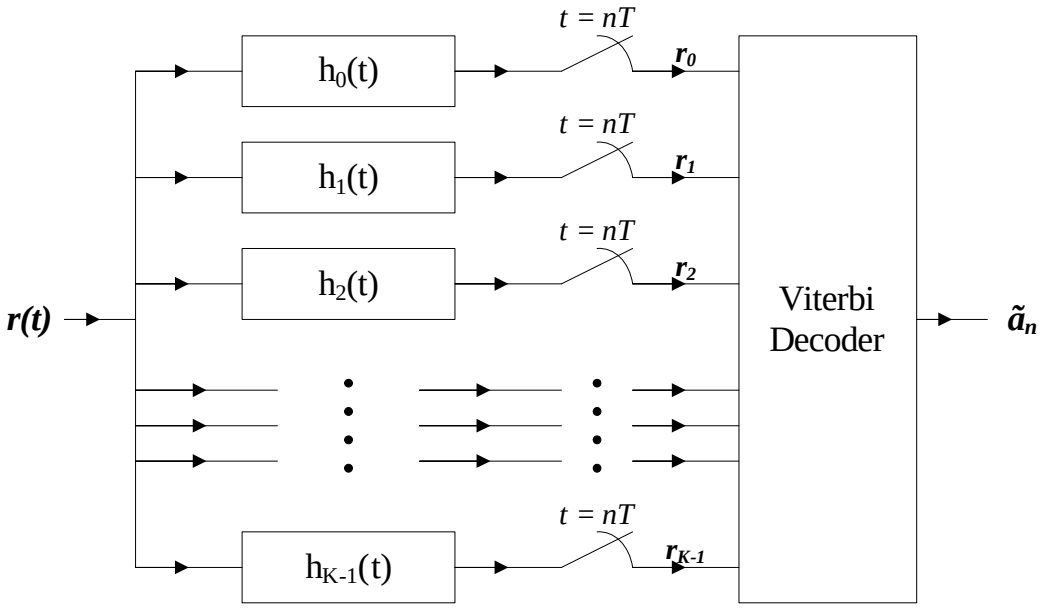

Figure 5.3: Optimum Receiver used in BER simulations

Optimum CPM receiver is illustrated in Figure 5.3. As shown in the figure, the receiver comprises of two main blocks: a matched filter bank, and a Viterbi decoder. The received signal $r(t)$ is welcomed by a bank of matched filters first. Then the outputs of these matched filters are sampled at every symbol period to generate branch metrics to feed the Viterbi decoder block. Since this receiver is based on a detection process that employs CPM trellis structure, the number of matched filters is equal to the number of all possible branches in the trellis. Hence, there are a total of $K = P \cdot 2^L$ matched filters in the optimum receiver in Figure 5.3, where p is the number of phase states and L is the duration of the frequency pulse $g(t)$ in terms of symbol period T. In equation (3.11), it was shown that the branch (partial) metric $Z_n(\tilde{\boldsymbol{\alpha}}_{\boldsymbol{n}}\tilde{\theta}_n)$ for baseband domain is,

$$Z_n(\tilde{\boldsymbol{\alpha}}_{\boldsymbol{n}}, \tilde{\theta}_n) = \mathbf{Re}\left\{ \int_{nT}^{(n+1)T} r(t) e^{-j[\theta(t,\tilde{\boldsymbol{\alpha}}_{\boldsymbol{n}}) + \tilde{\theta}_n]} dt \right\} \tag{5.12}$$

where $(\tilde{\boldsymbol{\alpha}}_{\boldsymbol{n}}, \tilde{\theta}_n)$ represent all the possible sequences in trellis, $\tilde{\boldsymbol{\alpha}} = (\tilde{\alpha}_n, \tilde{\alpha}_{n-1}, \cdots, \tilde{\alpha}_{n-L+1})$ and $\tilde{\theta}_n$ is a possible phase state which can have P different values. Hence, matched filters used in the optimum CPM receiver can be defined as,

$$\begin{aligned} h_k(t) &= e^{-j[\theta(t,\tilde{\boldsymbol{\alpha}}_{\boldsymbol{n}})+\tilde{\theta}_n]} \\ &= cos[\theta(t,\tilde{\boldsymbol{\alpha}}_{\boldsymbol{n}}) + \tilde{\theta}_n] - j\sin[\theta(t,\tilde{\boldsymbol{\alpha}}_{\boldsymbol{n}}) + \tilde{\theta}_n] \end{aligned} \tag{5.13}$$

Outputs of the matched filters are then used in Viterbi decoder as branch metrics to calculate the recursive summation in equation (5.11), and finally select the surviving sequence that maximizes $J_n(\tilde{\boldsymbol{\alpha}})$. This sequence is given out as the *received bits*.

5.2.3.2 LD (LAURENT DECOMPOSITION) BASED CPM RECEIVER

In Chapter 2 and [7], it has been shown that CPM signals can be represented as a linear combination of some amplitude modulated pulses, which is called Laurent Decomposition. The ability of composing a nonlinear CPM signal by a linear combination of real PAM signals comes with a different aspect for the receiver side. The receiver structure based on Laurent Decomposition is discussed in Chapter 3. In Figure 5.4, the structure of an LD Based CPM Receiver is illustrated. The main differences that are noticed immediately are the filter bank that differ from the Optimum CPM Receiver based on trellis structure and a new block called *Branch Metric Computer*.

In LD Based Receivers, the filters residing in the filter bank are matched to *Laurent pulses* $c_k(t)$, where $c_k(t)$ are the real pulses that constitute the transmitted signal. In Chapter 2 equation (2.10), it has been shown that

$$s(t,\boldsymbol{\alpha}) = \sum_{k=0}^{2^{L-1}-1} \sum_{n=0}^{N-1} b_{k,n} c_k(t-nT)$$

Hence, using $c_k(-t)$ as matched filters and filtering the receiver signal and then sampling at symbol period nT gives $r_{k,n}$ metrics, which have been previously defined in equation (3.17) as,

$$r_{k,n} = \int_{-\infty}^{\infty} r(t)c_k(t-nT)dt = r(t) \otimes c_k(-t)|_{t=nT}$$

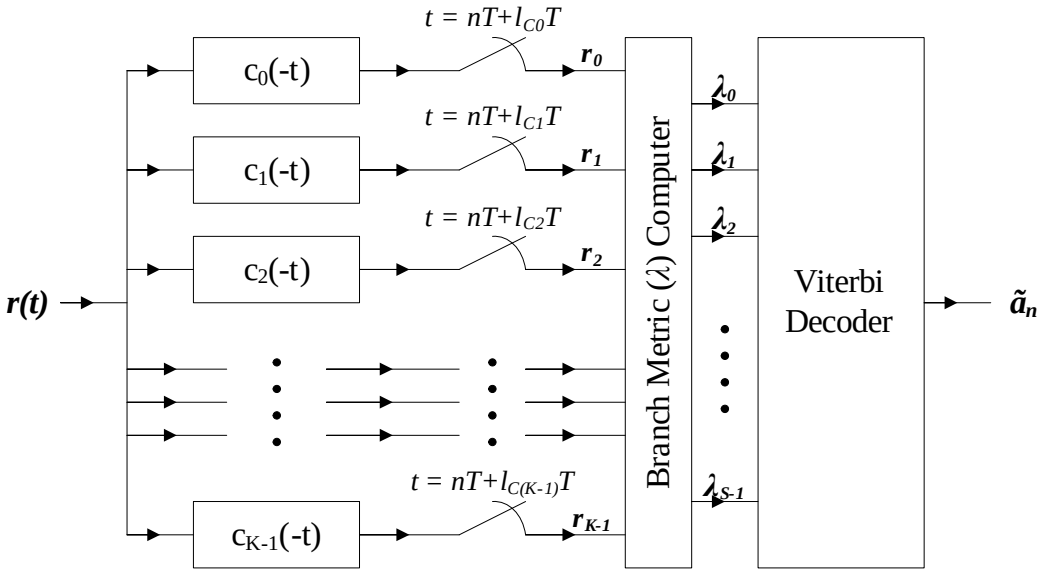

Figure 5.4: LD Based Receiver used in BER simulations

Then these metrics, $r_{k,n}$ are taken into the *Branch Metric Computer* block to be processed according to equation (3.18) which is reexpressed below,

$$\lambda_n = \mathbf{Re}\left\{\sum_{k=0}^{2^{L-1}-1} r_{k,n} b_{k,n}^*\right\}$$

to produce the branch metrics. Finally, these branch metrics are fed into the Viterbi decoder block and the surviving sequence which maximizes

$$\mathbf{Re}\left\{\int r(t)s^*(t,\boldsymbol{\alpha})dt\right\} = \sum_n \lambda_n$$

is selected and given out as the *received bits*.

5.2.4 MODEL VERIFICATION WITH MSK

After introducing the simulation models to be used in receiver error performance measurements, first we have to be sure that the models are correctly designed. So, we have used the well-known Minimum Shift Keying (MSK) modulation scheme to verify the models.

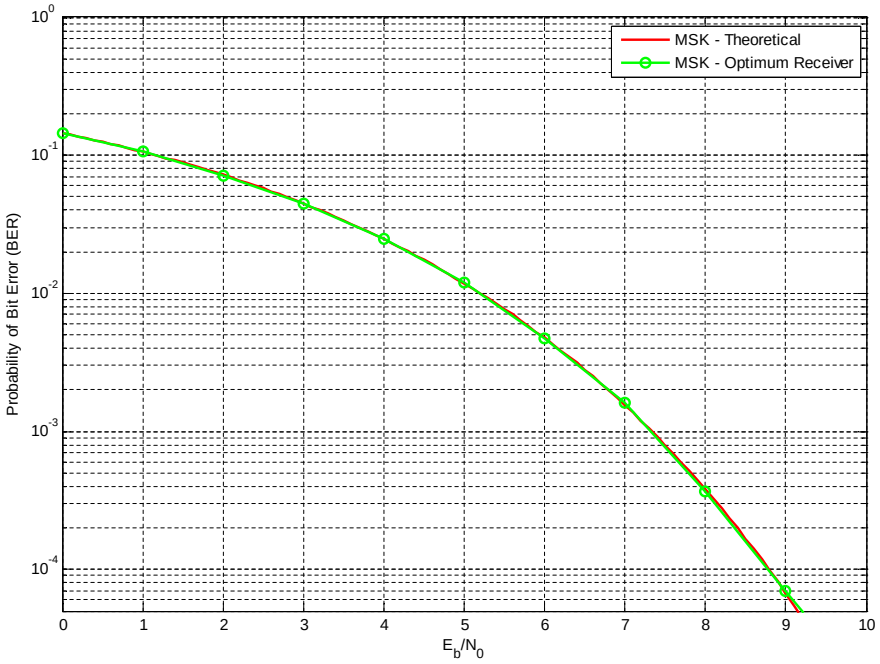

Figure 5.5: BER Curve for MSK - Optimum Receiver

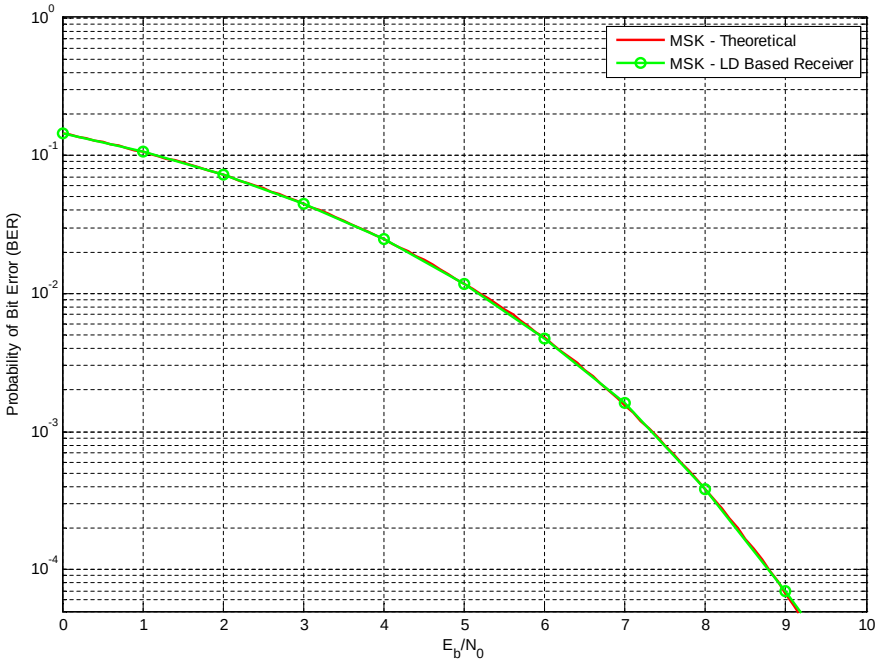

Figure 5.6: BER Curve for MSK - LD Based Receiver

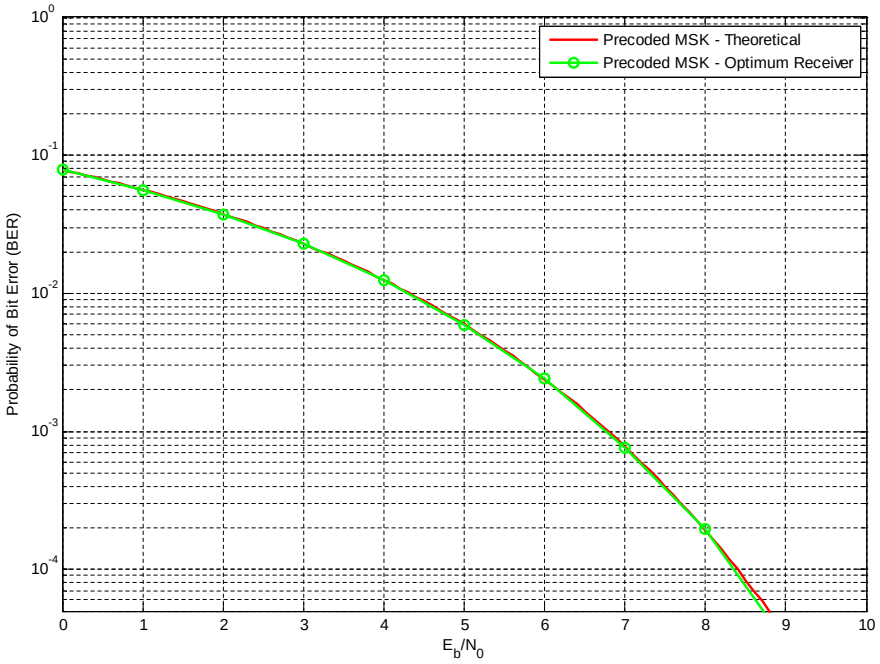

Figure 5.7: BER Curve for Precoded MSK - Optimum Receiver

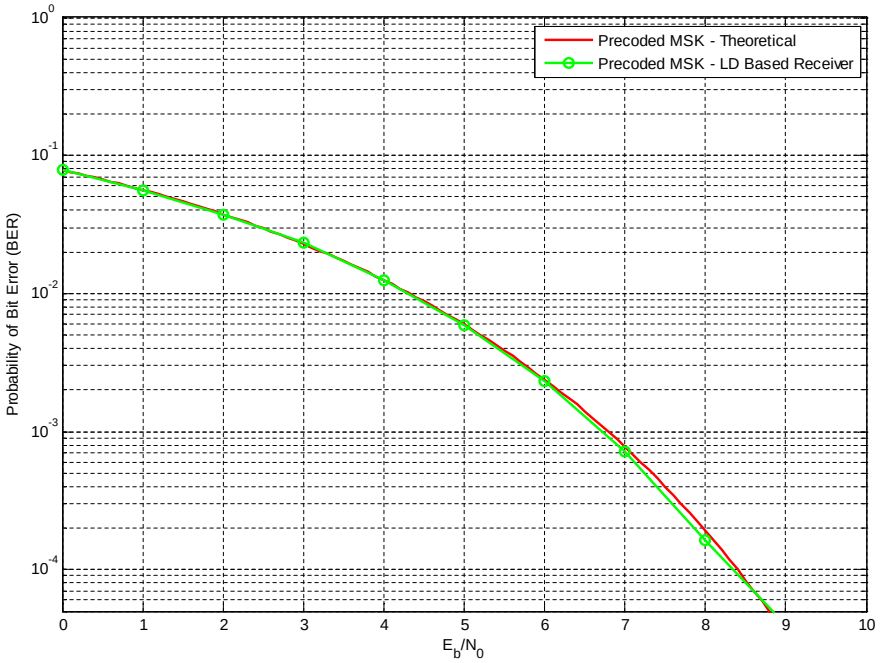

Figure 5.8: BER Curve for Precoded MSK - LD Based Receiver

A rectangular pulse shape with duration $L = 1$ and modulation index $h = 0.5$ is modulated using randomly generated data bits at transmitter side and added noise at the AWGN channel. Then this noisy MSK signal is fed to both receivers to measure their error performances. Figures 5.5 and 5.6 show BER versus E_b/N_0 graphs for optimum CPM receiver and LD based receiver employing conventional MSK, respectively.

In figures 5.7 and 5.8, error probability for *precoded* MSK is given. Precoded MSK is generated by adding a *precoder* between the data and the transmitter, and a *decoder* to the output of the receiver. Precoding is used in MSK systems that employ phase modulators to achieve the same error probability with BPSK. Conventional MSK has 3dB poorer error performance than BPSK modulation. Precoding used here is defined as the inverse operation for differential encoding, which is the differential decoder, [12]. The precoder block encodes the input data according to the following equation,

$$d_k = b_k \oplus b_{k-1} \tag{5.14}$$

The decoder used in the receiver side is then the well-known differential encoder, [12],

$$b_k = d_k \oplus b_{k-1} \tag{5.15}$$

With the use of precoding process defined herein, the implicit differential encoding that resides in the nature of CPM transmitters is eliminated for the MSK case, [12].

5.3 PERFORMANCE OF OPTIMUM GMSK RECEIVER FOR GSM

In Section 5.4, some receivers have been proposed for the new pulse shapes found in [5]. The advantage of these new pulse shapes is their superiority to the GSM modulation scheme when used with some particular modulation index values. The measure of their superiority is the gain in the amount of power needed to maintain the same probability of error. Since GMSK with $BT = 0.3$ and $h = 0.5$, which is the standard modulation scheme used in GSM, is employed as a reference to these performance measures in [5], it is also used as a reference for the comparison of the bit error rate performance characteristics of the receivers proposed in this thesis.

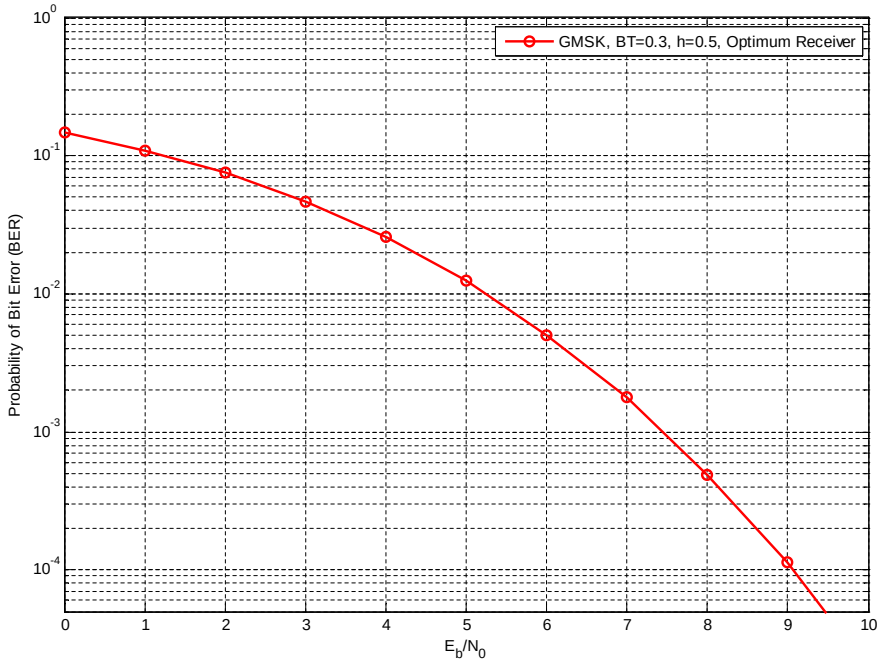

Figure 5.9: BER Curve for the GMSK Scheme ($BT = 0.3$, $h = 0.5$, $L_t = 7$) Used in GSM - Optimum Receiver

In Figure 5.9, the error performance of the optimum receiver based on phase trellis structure for GMSK ($BT = 0.3$, $h = 0.5$) is given. In the next section, this graph will be used as a reference.

5.4 PROPOSED RECEIVERS FOR NEW PULSE SHAPES

In [5], which is summarized in Chapter 4, two pulse shapes are introduced that are optimized to have better minimum Euclidean distance values with the constraint that the power spectral density of the pulse shapes should remain under GSM spectral envelope. The optimized pulse shapes have lengths of $L = 3$ and $L = 7$ symbol intervals. Using these pulse shapes in a digital communication system employing continuous phase modulation brings the advantage of 1.08dB ($L = 3$) or 2.3dB ($L = 7$) better performance with respect to the standard GMSK modulation scheme ($BT = 0.3$, $h = 0.5$, $L_t = 7$) used in GSM.

To have the performance gain provided by the new pulse shapes of [5], they must be used with the optimized h values, which are 0.5870 and 0.8633 for the pulse shapes with $L = 3$ and $L = 7$, respectively. But these modulation index values are impractical to implement a CPM receiver with practical number of states. To have a finite number of states in the decoding section of a CPM receiver, the modulation index value should be one that can be written in the form $h = \frac{m}{p}$ where m and p are relatively prime integers. Since the denominator p of this rational number determines the phase state number, it is of vital importance to choose a small value of p to be practical. Therefore, a research of practical modulation index values, h, with small degradations from the aforementioned error rate performance gains should be done for both new pulse shapes in order to be able to propose practical receivers.

5.4.1 $L = 3$ CASE

As mentioned before, the first thing to do in this section is to approximate the modulation index values found in [5] to fit in $h = \frac{m}{p}$ form with small p values that will lead us to have a small number of phase states in the receivers. To realize this search, we have to put some constraints in order to have practical outputs.

Table 5.1: Practical Modulation Index Values for the Optimum Pulse Shape ($L = 3$)

h (mod. index)	% Error in h	m (numerator)	p (denominator)	# of Phase States
0.5714	1.14	4	7	7
0.6000	3.81	3	5	10
0.5455	5.63	6	11	11
0.6154	6.47	8	13	13
0.5333	7.73	8	15	15
0.6250	8.13	5	8	16

Hence, two constraints are used in this work. First one is that we limit the span of the modulation index values to 10% of the original modulation index value, which is 0.5870 for $L = 3$ case, to have a small degradation with respect to the optimum case. Second one is that the number of phase states is limited to 16 to be practical in receiver design. In the light of these constraints, the modulation index values that are found are given in Table 5.1, sorted according to the difference in value to the original h value.

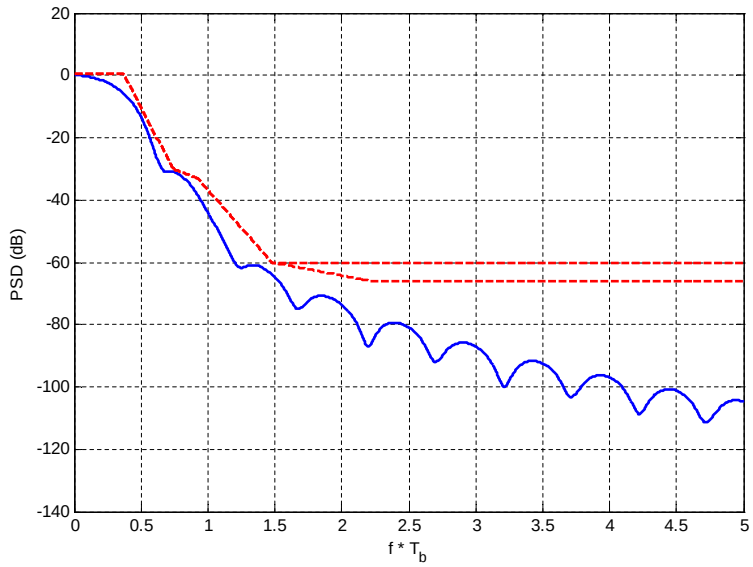

Figure 5.10: PSD of the Optimum Pulse Shape ($L = 3$) with $h = 4/7$

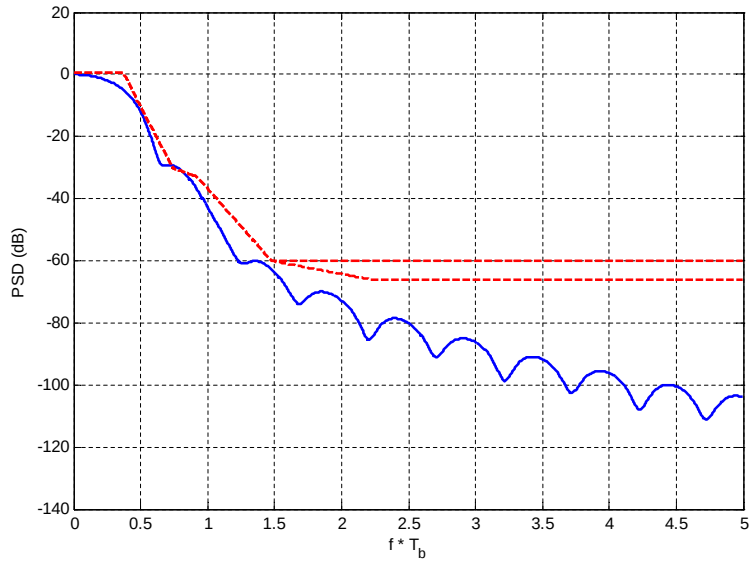

Figure 5.11: PSD of the Optimum Pulse Shape ($L = 3$) with $h = 3/5$

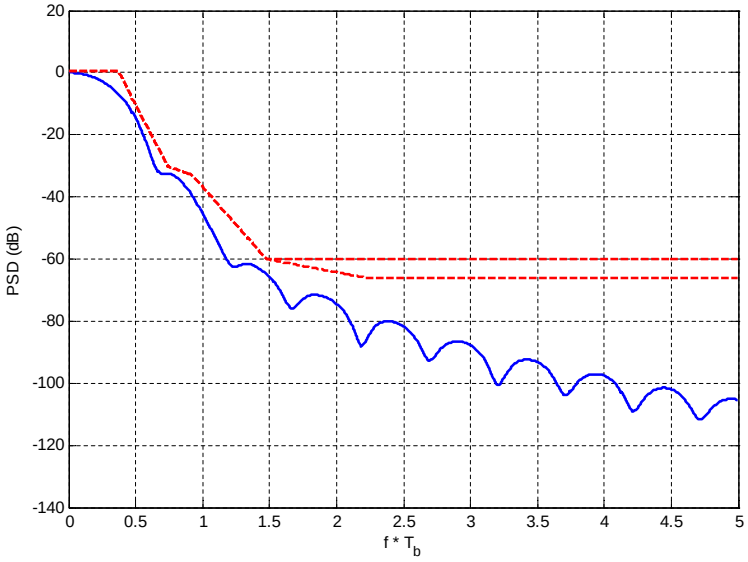

Figure 5.12: PSD of the Optimum Pulse Shape ($L = 3$) with $h = 6/11$

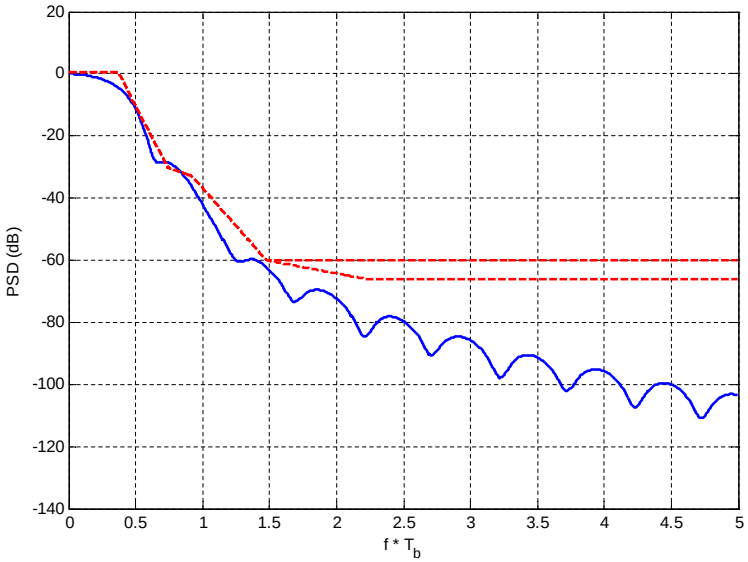

Figure 5.13: PSD of the Optimum Pulse Shape ($L = 3$) with $h = 8/13$

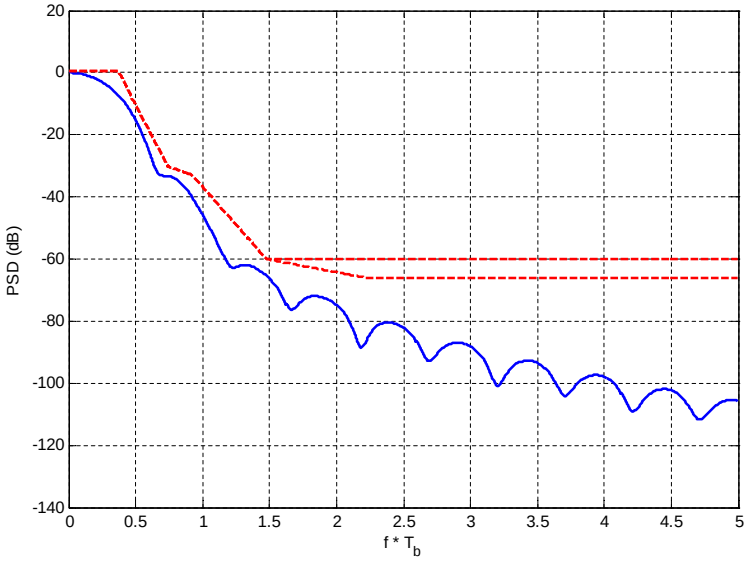

Figure 5.14: PSD of the Optimum Pulse Shape ($L = 3$) with $h = 8/15$

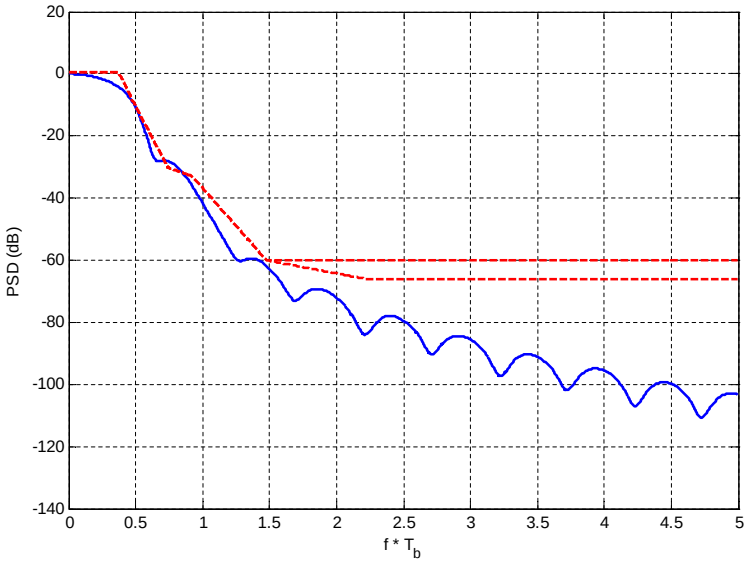

Figure 5.15: PSD of the Optimum Pulse Shape ($L = 3$) with $h = 5/8$

As shown in Table 5.1, we have found six modulation index values that differ from the original one by 10% max with the phase state number constraint of 16. But can any of these values violate the constraint that the power spectrum density of the pulse shape should stay below GSM spectral envelope? In figures 5.10 to 5.15, PSD of the pulse shapes with the modulation indices given in Table 5.1 are depicted to see whether the constraint is still maintained or not.

When the PSDs in figures 5.11, 5.13 and 5.15 are examined carefully, it can be seen that there is a violation of GSM spectral envelope between the normalized frequency ($f \cdot T_b$) values of 0.5 and 1, near the second bending point of the envelope. So, the modulation index values causing the optimum pulse shape to deteriorate the GSM spectral envelope constraint are not appropriate to be used indeed. Then the number of modulation indices decreases to three that satisfy all constraints.

The differences between the appropriate modulation indices found and the optimum one are 1.14%, 5.63% and 7.73%. These differences in values will lead to a degradation in the performance gain of the optimum case, which is calculated as 1.08dB in [5] with respect to the GMSK modulation scheme used in GSM. In the optimum case with $h = 0.5870$, the minimum squared Euclidean distance is 2.2287 where it is 1.7363 for the GSM modulation scheme. When the minimum squared Euclidean distance values are calculated according to the flowchart given in [5], [2], the results in Table 5.2 are obtained.

Table 5.2: Appropriate Modulation Indices for the Optimum Pulse Shape ($L = 3$)

h (mod. index)	% Error in h	m (num.)	p (denom.)	# of Phase States	d^2_{min}	Power Gain (dB)
0.5714	1.14	4	7	7	2.1485	0.93
0.5455	5.63	6	11	11	2.0120	0.64
0.5333	7.73	8	15	15	1.9473	0.50

In the condition where the channel is an AWGN channel and for large SNR values, the probability of an erroneous detection of a transmitted bit is approximated by,

$$P_e \approx K_{d_{min}} \cdot Q\left(\left(d_{min}^2 \frac{E_b}{N_0}\right)^{1/2}\right) \tag{5.16}$$

So, an increase in the value of minimum squared Euclidean distance, d_{min}^2, will cause less power to be used to have the same probability of error, because they are inversely proportional. Then the gain (in dB) in the amount of power needed can be calculated with

$$GAIN = 10log\left(\frac{d_{min}^2}{1.7363}\right) \tag{5.17}$$

where 1.7363 is the minimum squared Euclidean distance for GSM. After substitution of the minimum squared Euclidean distance values in Table 5.2 into equation (5.17), a gain of 0.93dB, 0.64dB and 0.50dB is obtained by using the modulation indices $h = 4/7$, $h = 6/11$ and $h = 8/15$, respectively. It is not so surprising that the power gain decreases as the distance in h values to the optimum case increases. Looking at the power gains in Table 5.2, it is obvious that the best receiver performance will occur with modulation index $h = 4/7$. However, it will be better to see the performance with all three modulation indices, because the best case with $h = 4/7$ may be worse than the others in some situations when complexity reduction is applied.

The bit error rate performance of the optimum receiver designed for the optimum pulse shape ($L = 3$) with modulation index of $h = 4/7$ is depicted in Figure 5.16. This receiver, which is based on phase trellis structure as shown in Figure 5.3, has $P \cdot 2^L = 56$ matched filters in the filter bank, where $P = 7$ is the phase state number and $L = 3$ is the pulse shape duration in symbol intervals. The filters accept the received noisy baseband CPM signal as inputs and produce the branch metrics to be used in Viterbi decoder section. There are $P \cdot 2^{L-1} = 28$ states to be processed in the Viterbi algorithm processor. In Figure 5.16, the gain in amount of power with respect to GSM modulation scheme can be seen. For probability of error $P_e = 10^{-4}$, the gain is a little bit smaller than 1dB in this simulation result. That confirms the calculated power gain of 0.93dB for that modulation index.

After verification of the amount of power gain for $h = 4/7$ with optimum MLSE receiver based on phase trellis, now it is turn to propose some simpler receivers. In Figure 5.17, the

simulated performance of the LD (Laurent Decomposition) based receiver is given. This receiver contains only $2^{L-1} = 4$ matched filters in the filter, with no state reduction process, where $Q = L = 3$ is taken. The metrics computed by these filters are preprocessed by the *partial metric computer* to produce $P2^L = 56$ branch metrics for the VA processor which have $P \cdot 2^{L-1} = 28$ states. As it might be guessed, even using LD based receiver with no state reduction leads to a decrease in the number of matched filters with no degradation. The power gain is again close to 1dB as in the optimum receiver case.

In Figure 5.18, simulated error performances of reduced-state LD based receivers are given in addition to the optimal case of $Q = L = 3$. When examined carefully, it is obvious that there is almost no change in performance when $Q = L - 1 = 2$ is taken. The same gain in amount of power (≈1dB) is achieved with only $2^{Q-1} = 2$ matched filters in the filter bank and $P \cdot 2^{Q-1} = 14$ states in the Viterbi decoder section. For the case where $Q = L - 2 = 1$, there is a degradation in error performance, but it is still better than the GSM scheme *(GMSK, BT=0.3, h=0.5)*. So, using only one matched filter and only 7 states in Viterbi decoding process with the optimum pulse shape ($L = 3$) and $h = 4/7$ gives better results (≈0.6dB) than

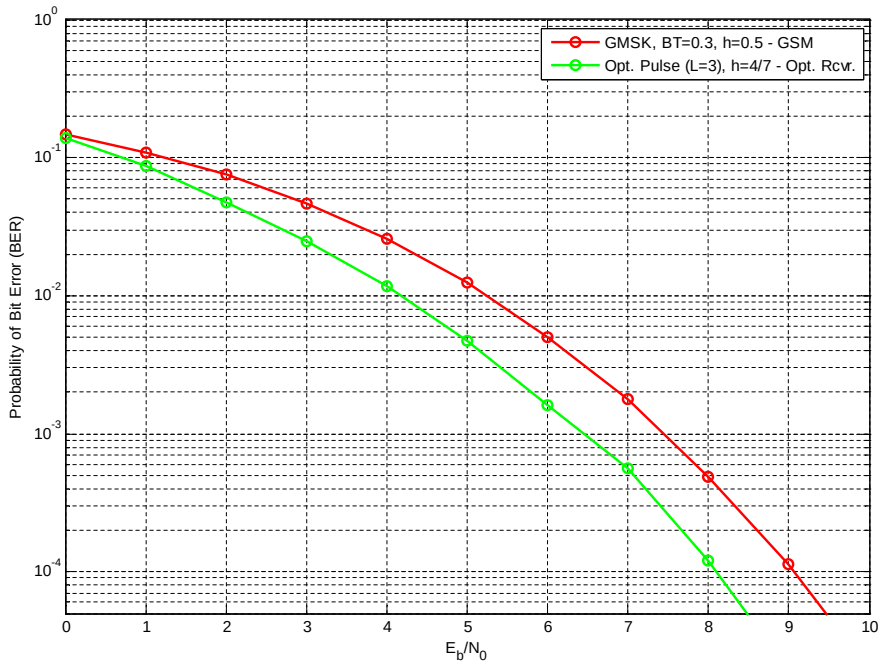

Figure 5.16: BER Curve for the Optimum Pulse Shape ($L = 3$) with $h = 4/7$ - Optimum Receiver

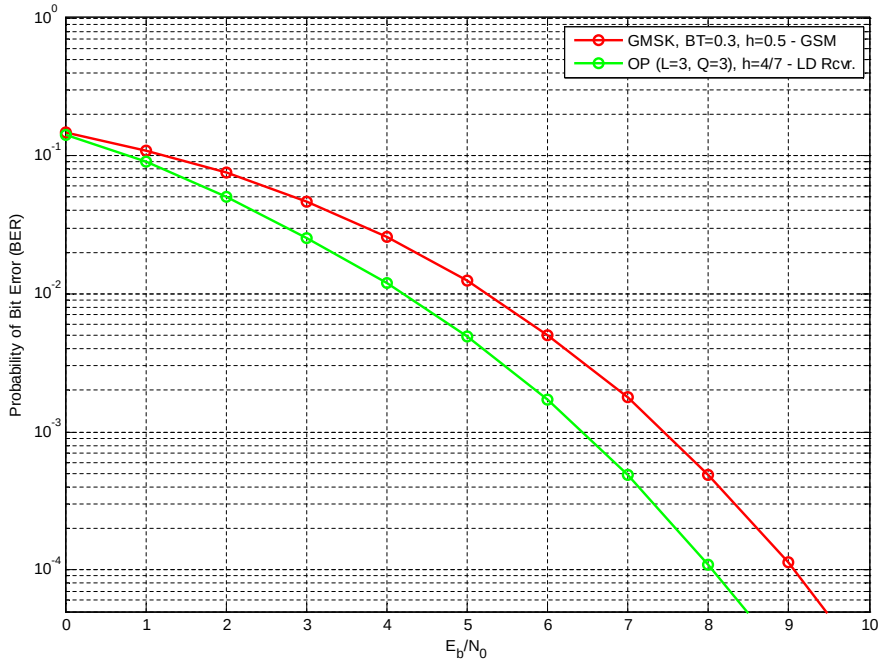

Figure 5.17: BER Curve for the Optimum Pulse Shape ($L = 3$) with $h = 4/7$ - LD Based Receiver with $Q = L = 3$

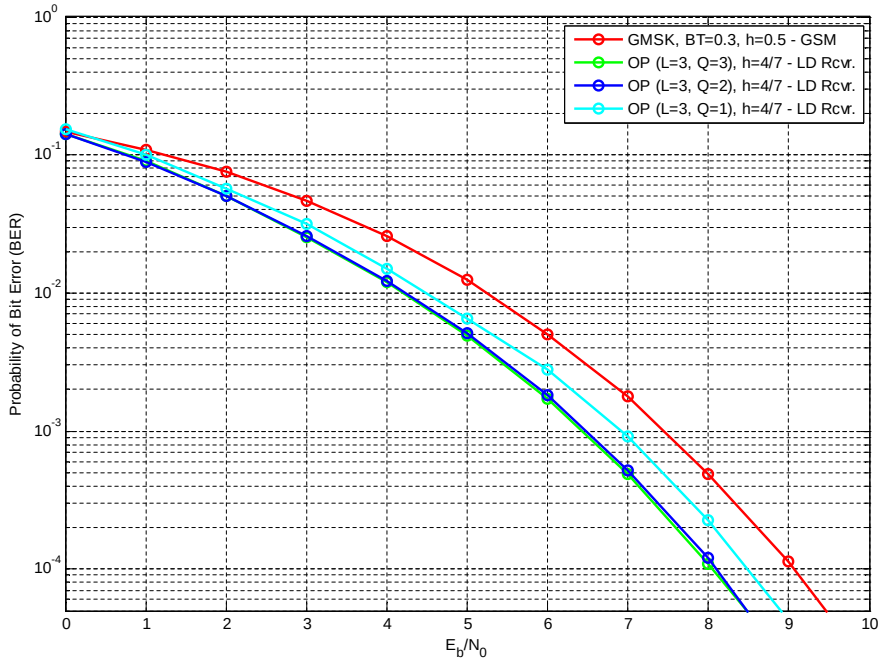

Figure 5.18: BER Curve for the Optimum Pulse Shape ($L = 3$) with $h = 4/7$ - LD Based Receiver with $Q = 3$, $Q = 2$ and $Q = 1$

the standard GSM modulation scheme.

Bit error rate performance graphs for the receivers designed for the optimum pulse shape with modulation index of $h = 6/11$ are given in figures 5.19 to 5.21. Figure 5.19 illustrates the optimum MLSE receiver case that is based on phase trellis structure. This receiver consists of 88 matched filters, where the phase state count is 11 this time. The branch metrics computed by the matched filters are used to feed a 44-state Viterbi processor that decodes received data bits. At $P_e = 10^{-3}$ and $P_e = 10^{-4}$, the gain with respect to the GMSK signal is about 0.6-0.7dB. The theoretical value is calculated as 0.64dB. In Figure 5.20, the performance of LD based receiver with no state reduction ($Q = L$) is depicted. The gain is again about 0.6-0.7dB, but this time 4 matched filters are used instead of 88 as in the optimum phase trellis based receiver. The number of states used in Viterbi algorithm processor is not changed; there are 44 states again.

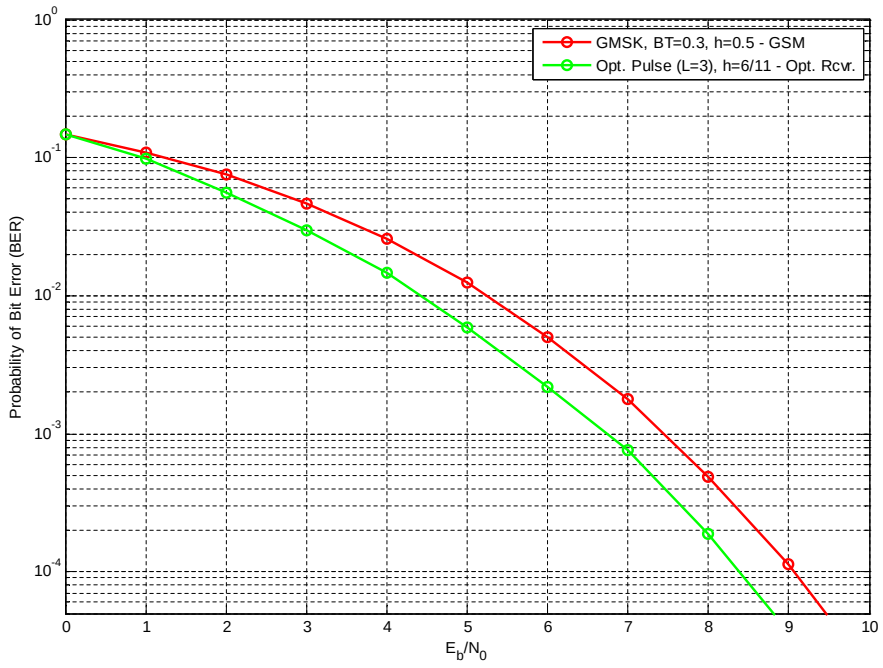

Figure 5.19: BER Curve for the Optimum Pulse Shape ($L = 3$) with $h = 6/11$ - Optimum Receiver

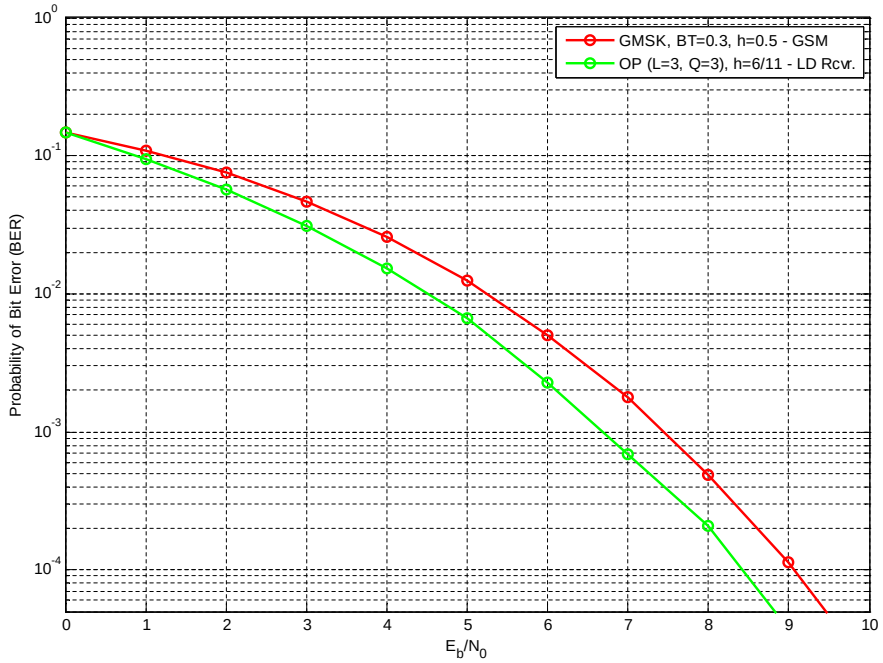

Figure 5.20: BER Curve for the Optimum Pulse Shape ($L = 3$) with $h = 6/11$ - LD Based Receiver with $Q = L = 3$

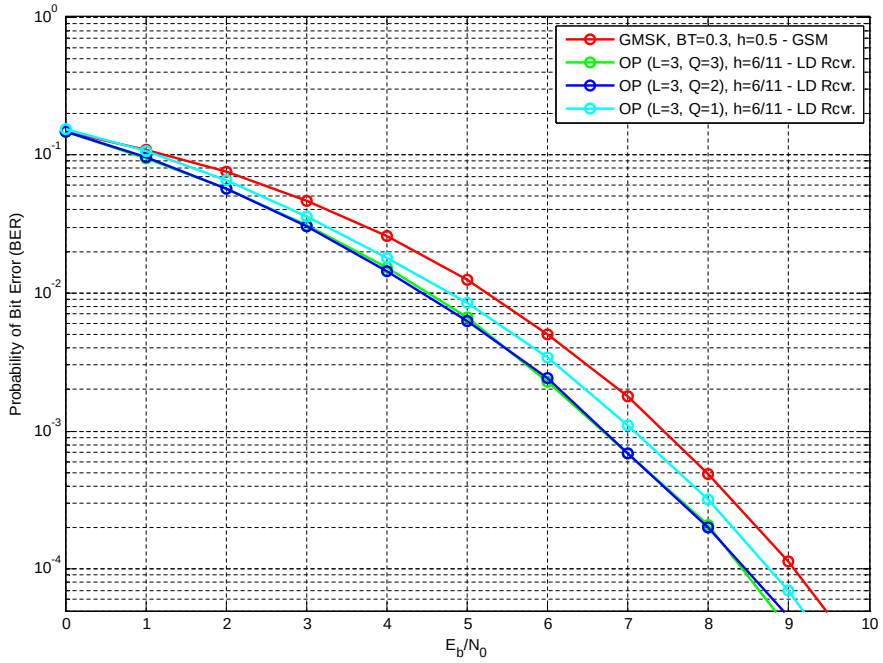

Figure 5.21: BER Curve for the Optimum Pulse Shape ($L = 3$) with $h = 6/11$ - LD Based Receiver with $Q = 3$, $Q = 2$ and $Q = 1$

In Figure 5.21, reduced-state LD based receivers in addition to the LD based receiver with no state reduction is illustrated for modulation index of $h = 6/11$. When $Q = L - 1 = 2$, only 2 matched filters are used in the receiver, resulting in 22 states in Viterbi decoding process. Performance of this receiver is almost the same with the optimum case. But when $Q = L - 2 = 1$ is taken for state reduction, a degradation of about 0.3dB is introduced to the system. But the performance is still better than the modulation scheme used in GSM and the matched filter count is only one, leading to only 11 states in Viterbi decoder.

The performance of the optimum receiver designed for the optimum pulse shape with duration $L = 3$ and modulation index $h = 8/15$ is given in Figure 5.22. The filter bank of this receiver consists of $P \cdot 2^L = 120$ matched filters and it has a Viterbi decoding processor running on $P \cdot 2^{L-1} = 60$ states. Power gain achieved by the usage of optimum pulse shape with this modulation index is about 0.4-0.5dB at the probability of error $P_e = 10^{-3}$ as the figure shows. The theoretical result is 0.5dB.

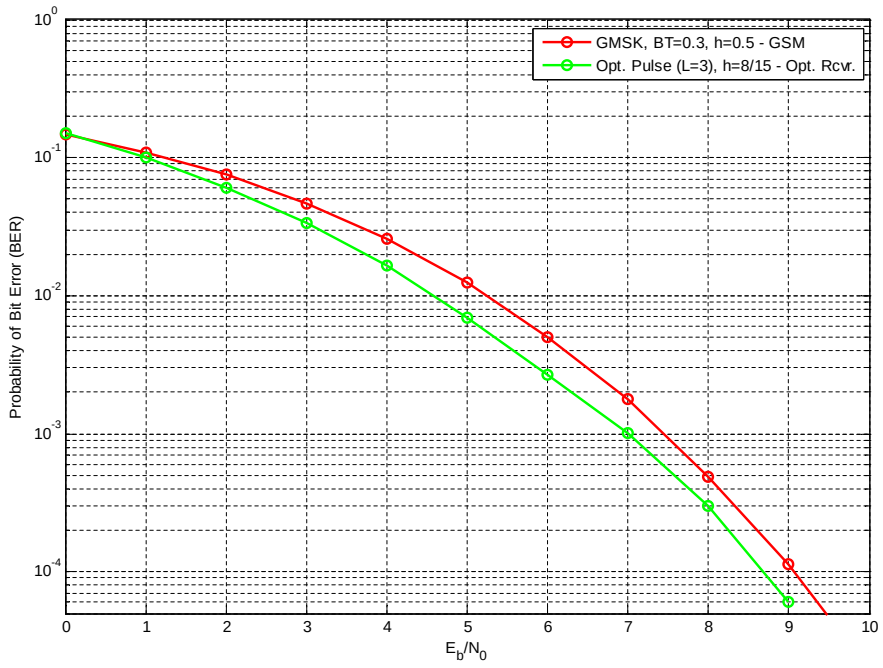

Figure 5.22: BER Curve for the Optimum Pulse Shape ($L = 3$) with $h = 8/15$ - Optimum Receiver

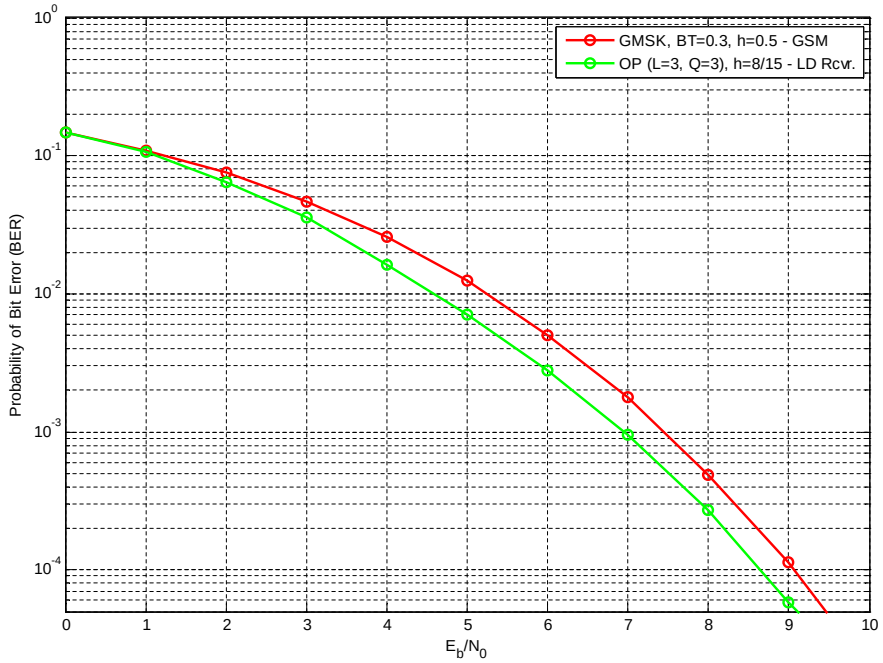

Figure 5.23: BER Curve for the Optimum Pulse Shape ($L = 3$) with $h = 8/15$ - LD Based Receiver with $Q = L = 3$

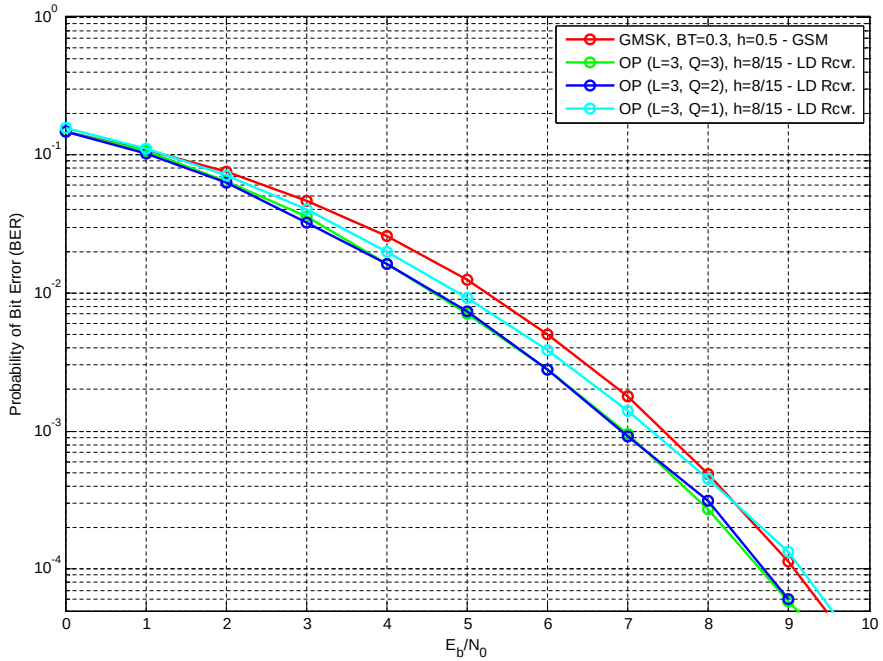

Figure 5.24: BER Curve for the Optimum Pulse Shape ($L = 3$) with $h = 8/15$ - LD Based Receiver with $Q = 3$, $Q = 2$ and $Q = 1$

In figures 5.23 and 5.24, LD based receiver performances for $h = 8/15$ are shown. Figure 5.23 shows the receiver with no state reduction ($Q = L = 3$), and Figure 5.24 gives the receiver error performances before and after state reduction applied. Without applying state reduction, the number of matched filters is equal to 4, where the number of states is 60 as in the optimum case. The gain with respect to GSM scheme is about 0.5dB. After applying state reduction techniques, matched filter number for $Q = L - 1 = 2$ is 2 resulting in 30 states in Viterbi decoder; and for $Q = L - 2 = 1$ case, only one matched filter is used with 15 states in Viterbi decoder. The gain in amount of power needed to have the same probability of error for high SNR values is almost the same for $Q = 2$; but when $Q = 1$ is used, the performance of the receiver is not better than the standard GSM modulation scheme.

5.4.2 $L = 7$ CASE

This section begins with approximating the modulation index values for the optimum pulse shape with pulse duration $L = 7$ symbol intervals as in the previous section it is done for $L = 3$ case. The constraints are the same, too; the span of the modulation index values is limited to 10% of the original modulation index value, which is 0.8633 this time for $L = 7$ case, and the number of phase states is limited to 16. Conforming this limitations, the modulation index values found for the optimum pulse shape with duration $L = 7$ are given in Table 5.3, sorted according to the difference in value to the optimum h value.

Table 5.3: Practical Modulation Index Values for the Optimum Pulse Shape ($L = 7$)

h (mod. index)	% Error in h	m (numerator)	p (denominator)	# of Phase States
0.8571	0.71	6	7	7
0.8750	1.36	7	8	16
0.8889	2.96	8	9	9
0.8333	3.47	5	6	12
0.9091	5.30	10	11	11
0.9231	6.92	12	13	13
0.8000	7.33	4	5	5
0.9333	8.11	14	15	15

As shown in Table 5.3, we have found eight modulation index values for the optimum pulse shape with duration $L = 7$. In figures 5.25 to 5.32, PSD of the pulse shapes with the

modulation indices given in Table 5.3 are depicted to see whether the constraints are still maintained or not.

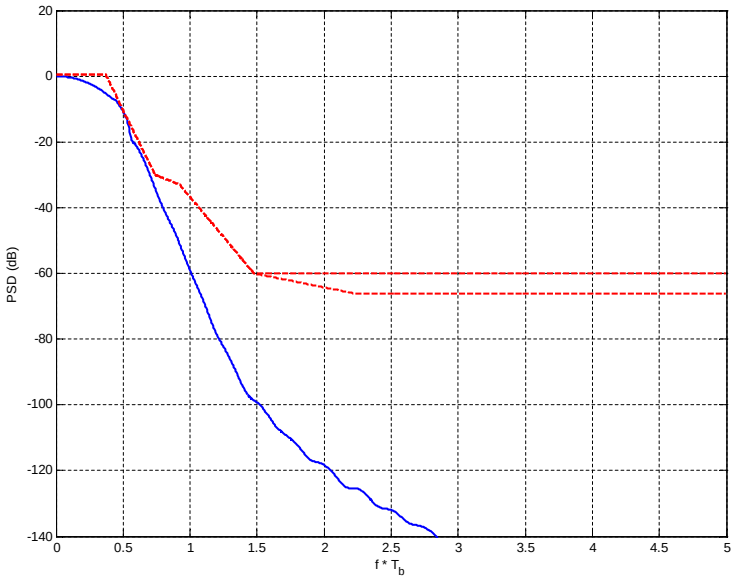

Figure 5.25: PSD of the Optimum Pulse Shape ($L = 7$) with $h = 6/7$

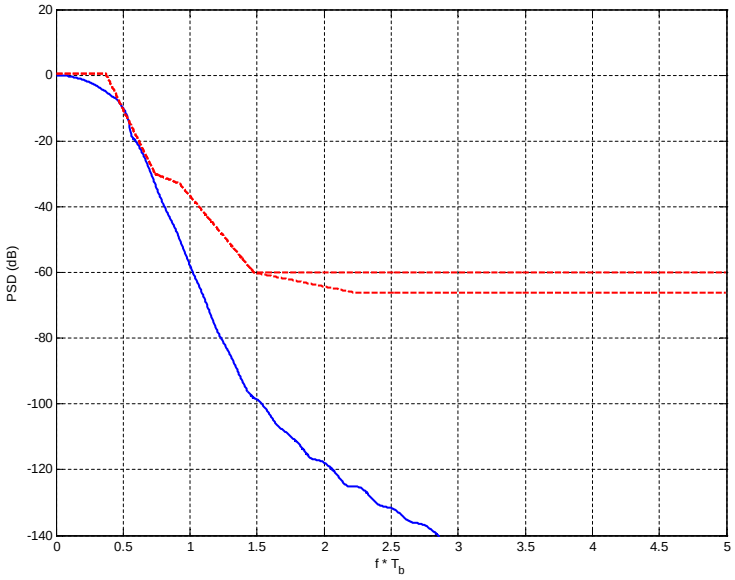

Figure 5.26: PSD of the Optimum Pulse Shape ($L = 7$) with $h = 7/8$

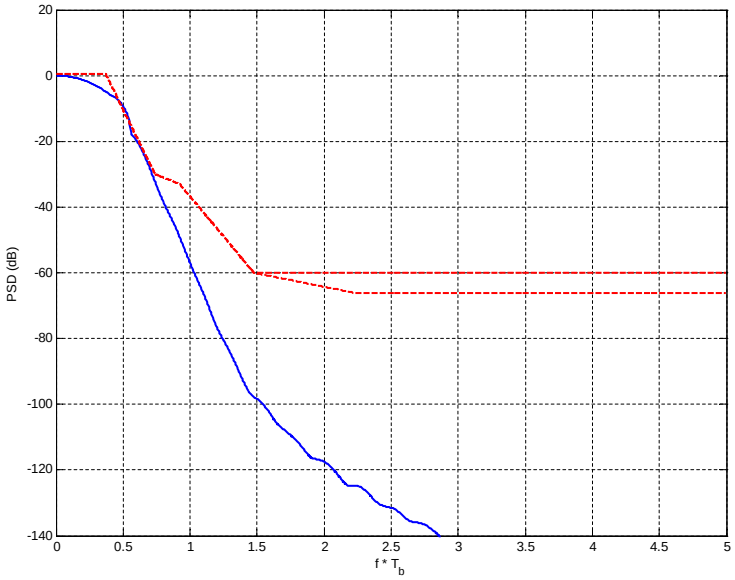

Figure 5.27: PSD of the Optimum Pulse Shape ($L = 7$) with $h = 8/9$

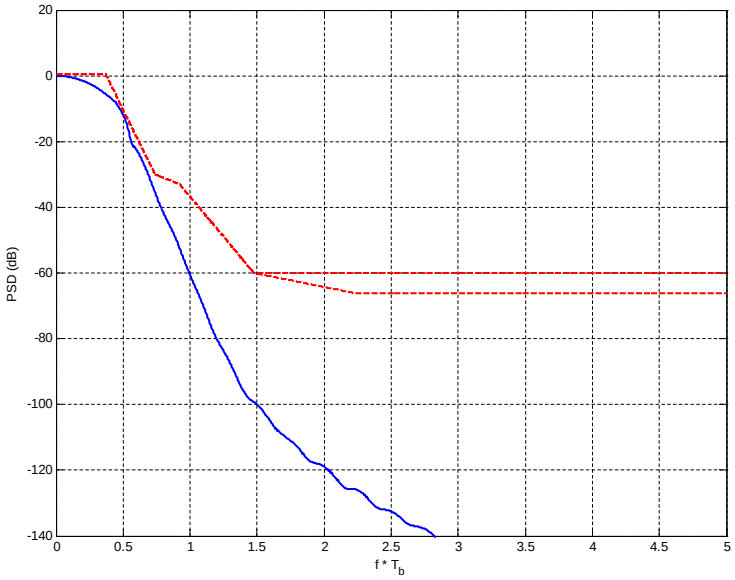

Figure 5.28: PSD of the Optimum Pulse Shape ($L = 7$) with $h = 5/6$

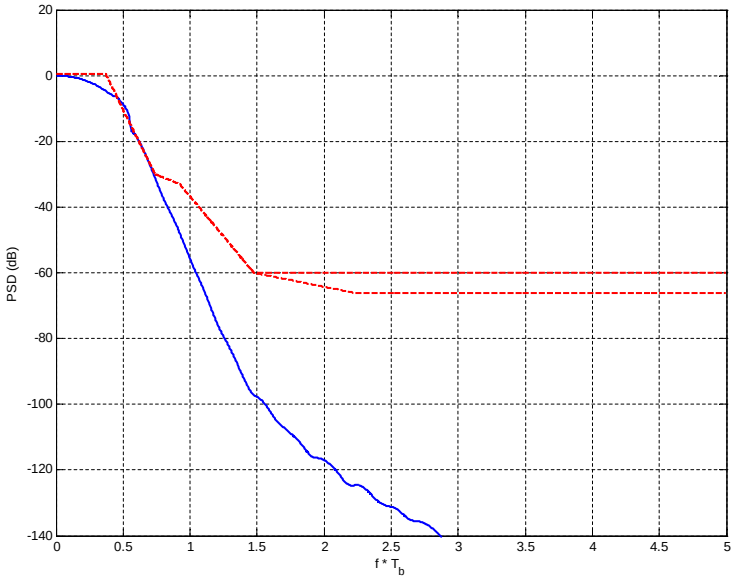

Figure 5.29: PSD of the Optimum Pulse Shape ($L = 7$) with $h = 10/11$

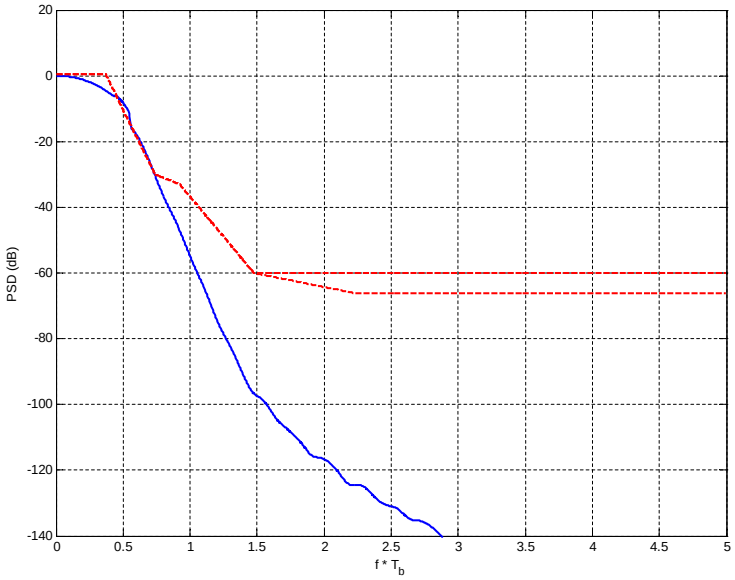

Figure 5.30: PSD of the Optimum Pulse Shape ($L = 7$) with $h = 12/13$

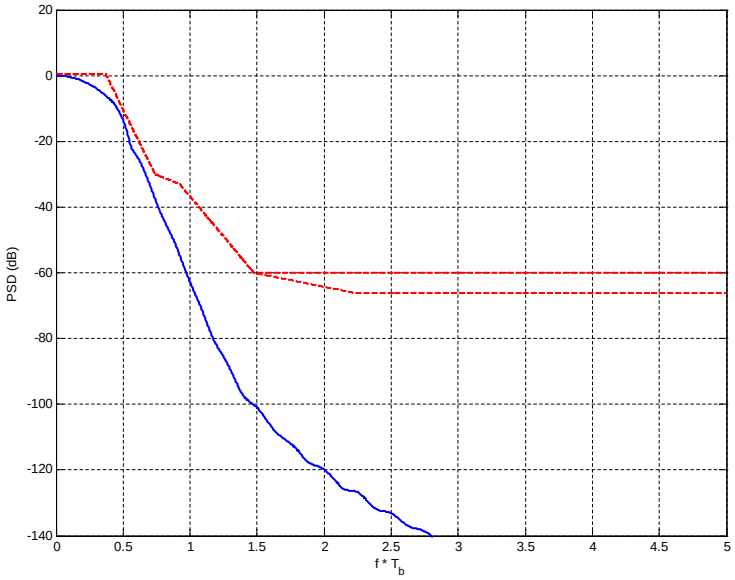

Figure 5.31: PSD of the Optimum Pulse Shape ($L = 7$) with $h = 4/5$

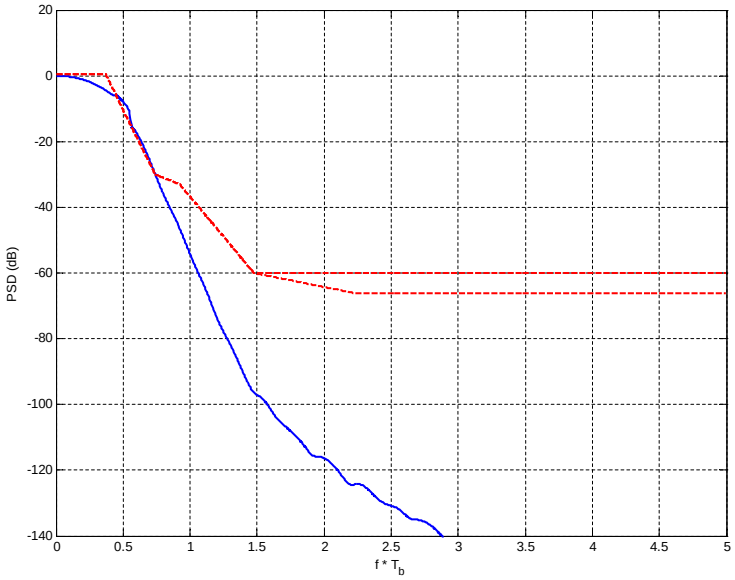

Figure 5.32: PSD of the Optimum Pulse Shape ($L = 7$) with $h = 14/15$

Figures 5.26, 5.27, 5.29, 5.30 and 5.32 show the optimum pulse shape ($L = 7$) power spectrum densities with modulation indices that cause violation of the GSM spectral envelope. Around the normalized frequency value $f \cdot T_b = 0.5$, these pulse shapes with modulation index values of 7/8, 8/9, 10/11, 12/13 and 14/15 deteriorate the constraint. Hence those modulation indices are not suitable to be used with the optimum pulse shape of length $L = 7$ symbol intervals. So the number of the possible modulation indices is three again.

The differences between the appropriate modulation indices found and the optimum one are 0.71%, 1.36% and 2.96%. These differences in values will lead to a degradation in the power gain of the optimum case, which is calculated as 2.3dB in [5] with respect to the GMSK modulation scheme used in GSM. In the optimum case with $h = 0.8633$, the minimum squared Euclidean distance is 2.9450. When the minimum squared Euclidean distance values are calculated according to the flowchart given in [5], [2], the results in Table 5.4 are obtained.

Table 5.4: Appropriate Modulation Indices for the Optimum Pulse Shape ($L = 7$)

h (mod. index)	% Error in h	m (num.)	p (denom.)	# of Phase States	d^2_{min}	Power Gain (dB)
0.8571	0.71	6	7	7	2.9113	2.25
0.8333	3.47	5	6	12	2.7810	2.05
0.8000	7.33	4	5	5	2.5995	1.75

After substitution of the minimum squared Euclidean distance values in Table 5.2 into equation (5.17), a gain of 2.25dB, 2.05dB and 1.75dB is obtained by using the modulation indices $h = 6/7$, $h = 5/6$ and $h = 4/5$, respectively. Table 5.2 shows that the phase state count of the modulation scheme with $h = 5/6$ is 12, which is about two-fold of the others. Using modulation index $h = 6/7$ has lower phase state count and larger minimum squared Euclidean distance which makes it better in terms of error performance. There is a noticeable difference (about 0.5dB) in power gain between $h = 6/7$ and $h = 4/5$ cases, but phase state numbers are quite close to each other, which are 7 and 5 respectively. Since the length of the optimum pulse shape is quite long ($L = 7$) this time, bit error rate simulations also consume longer times. So, only the best case which is the closest one to the optimum value of h is examined in terms of error performance of receivers in this section, which uses modulation index $h = 6/7$.

As we have seen in the previous section, optimum receiver based on phase trellis structure and LD based receiver with no state reduction give the same results in terms of error performance, and LD based receiver comprises of less matched filters which is better in practice. So, in Figure 5.33, LD based receiver for the optimum pulse shape ($L = 7$) employing modulation index $h = 6/7$ is given. In this receiver Q is taken to be equal to $L = 7$, which means no state reduction exists. There are $2^{L-1} = 64$ matched filters in the filter bank and $P \cdot 2^{L-1} = 448$ states used in Viterbi decoder section. According to the BER curve in the figure, the gain in amount of power at $P_e = 10^{-3}$ or $P_e = 10^{-4}$ is measured to be ≈2.25dB, which conforms to the mathematical calculations.

In Figure 5.34, error performances of reduced-state LD based receivers for $Q = 6$ and $Q = 5$ are given. It is obvious that 2-fold or 4-fold reduction at matched filter and state numbers of the optimal LD based receiver does not cause any degradation in error performance. If we go on state reduction by two more steps, i.e. take $Q = 3$, the degradation in error performance becomes very large.

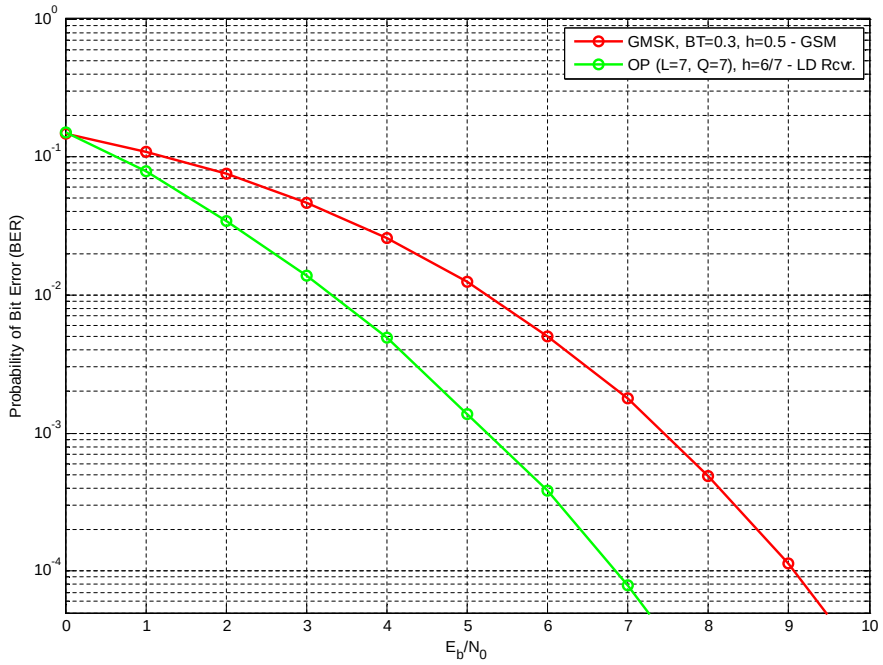

Figure 5.33: BER Curve for the Optimum Pulse Shape ($L = 7$) with $h = 6/7$ - LD Based Receiver with $Q = L = 7$

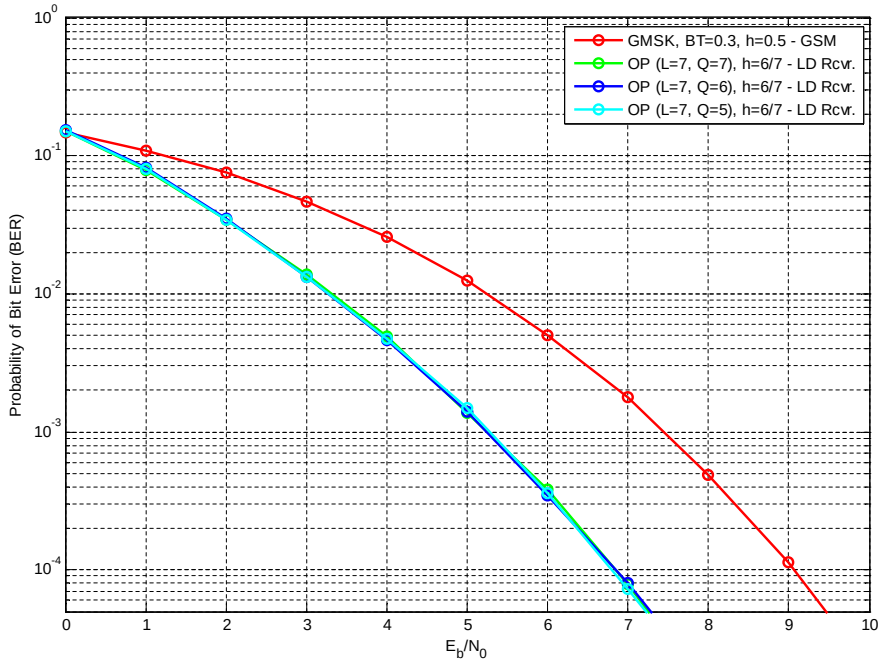

Figure 5.34: BER Curve for the Optimum Pulse Shape ($L = 7$) with $h = 6/7$ - LD Based Receiver with $Q = 7$, $Q = 6$ and $Q = 5$

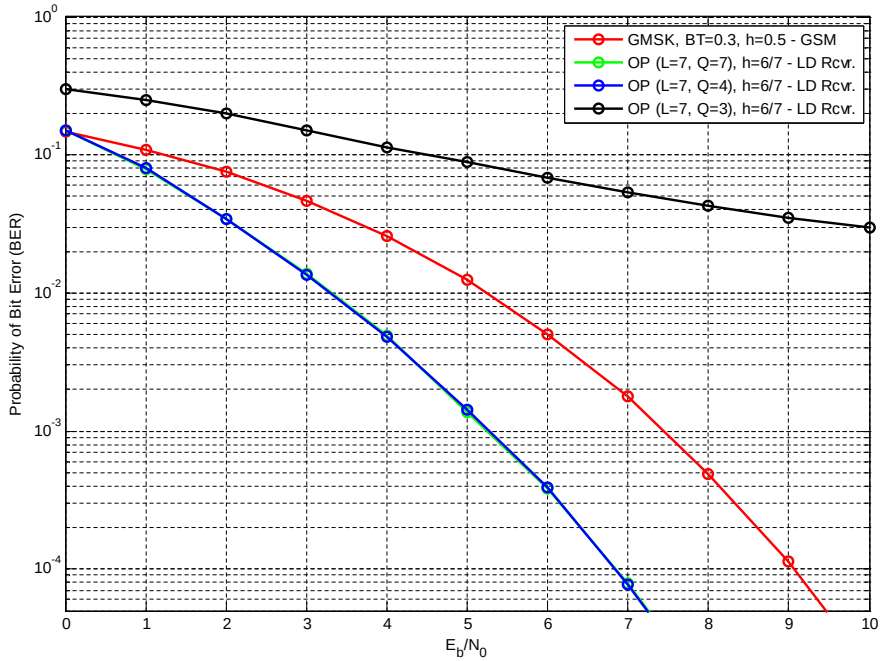

Figure 5.35: BER Curve for the Optimum Pulse Shape ($L = 7$) with $h = 6/7$ - LD Based Receiver with $Q = 7$, $Q = 4$ and $Q = 3$

In Figure 5.35, BER versus E_b/N_0 curves for $Q = 4$ and $Q = 3$ are depicted. For the case where Q is taken to be 4, the error performance is the same with the optimal case where $Q = L = 7$. But one step more state reduction makes the error performance even worse than the GMSK scheme used in GSM. Taking $Q = 3$ is not a right decision.

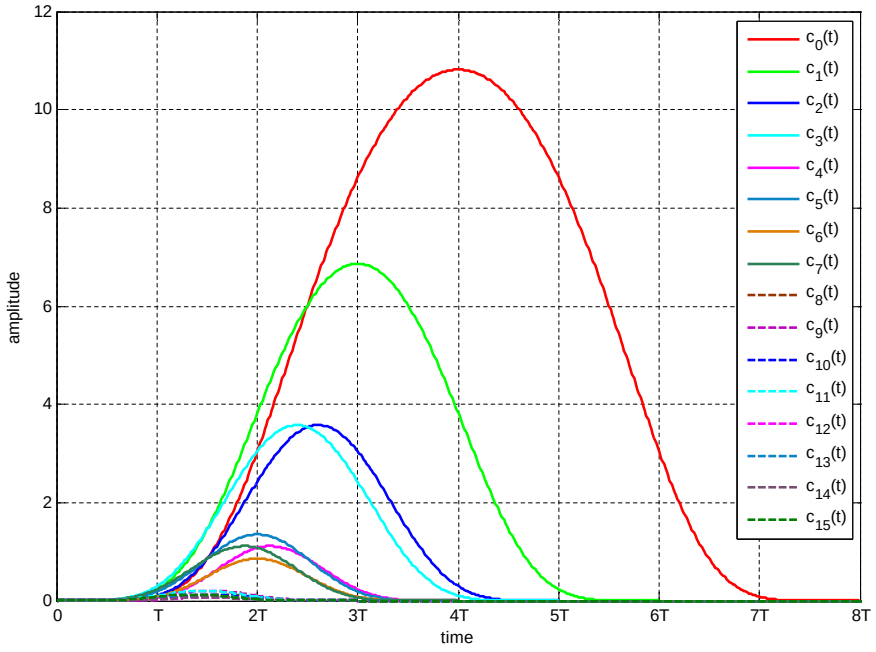

Figure 5.36: Laurent Pulses for the Optimum Pulse Shape with $L = 7$ and $h = 6/7$

First sixteen Laurent pulses are shown in Figure 5.36 for the optimum pulse shape with duration $L = 7$. It is clear that the energy is concentrated in the first eight pulses, from $c_0(t)$ to $c_7(t)$. The rest of the Laurent pulses are very small so that they are negligible in receiver implementation. Hence, using only 8 filters matched to first 8 Laurent pulses gives almost the same error performance with the optimal case.

Using less Laurent pulses instead of all actually causes the minimum Euclidean distance to decrease. Omitting pulses with negligible energy leads to an unnoticeable degradation. However, if a number of pulses having significant energy is omitted, then the degradation in minimum Euclidean distance becomes considerable. As the modulation index, h, gets larger and approaches to 1, the difference between the optimum case and the reduced-complexity

case gets larger, and the minimum Euclidean distance tends to zero at a point called *breakdown point*, [11], [22]. Hence, the reason of the abrupt change in BER curve transition from $Q = 4$ to $Q = 3$ case for the optimum pulse shape with $L = 7$ is the large modulation index ($h = 6/7$) used (see Figure 5.35). However, we have not seen such a situation for the optimum pulse shape with duration $L = 3$, even in the one matched filter case, because the modulation indices for $L = 3$ are close to 0.5. In [22], it is indicated that the performance of the reduced-complexity receiver is very close to the optimum case when $h \leq 0.5$.

Figures 5.34 and 5.35 show that the LD based receivers for $Q = 7$, $Q = 6$, $Q = 5$ and $Q = 4$ have the same error performances. Taking $Q = 4$ in this case, leads to the least matched filters and least number of states. By taking $Q = 4$, the receiver comprises of only $2^{Q-1} = 8$ matched filters and $P \cdot 2^{L-1} = 56$ states in Viterbi decoder, where $P = 7$ is the number of phase states determined by the modulation index's denominator. Since the receiver which $Q = 4$ is employed is the most simplified version of that scheme without causing any degradation, its usage seems to be the best for $L = 7$ and $h = 6/7$.

CHAPTER 6

CONCLUSION

In this thesis, the main goal has been to find a feasible receiver structure that provides a good error performance with acceptable degradation but affordable complexity, for the new pulse shapes expressed in [5], which is summarized in Chapter 4. These pulse shapes are optimized to give the best minimum squared Euclidean distance values under the constraint that their PSD should stay below GSM spectral envelope defined in [20]. However, the approach in [5] uses parameters that cause the number of states and matched filters to increase considerably, and thus yielding high complexity for receiver implementation.

Reducing the complexity of a CPM receiver governing MLSE and Viterbi algorithms can be divided into two classes. The first one is reducing the number of required matched filters in the filter bank. The second one is reducing the states used in the Viterbi decoder. For this purpose, after a survey about complexity reduction techniques employed in CPM area, receiver structures based on Laurent Decomposition that uses PAM representation of CPM signals is decided to go on within the study. This receiver structure permits both reducing the size of the matched filter bank and the state number in the Viterbi decoder at the same time, without causing a noticeable degradation. MATLAB software tool is used for implementation of receivers and performance simulations conducted throughout the study.

All the simulations have been conducted on baseband signals. To realize the objective of the study, three simulation blocks were implemented; a transmitter to create the CPM signal, an AWGN channel that adds noise to the transmitted signal and a receiver to decode the data bits. The performance of the receivers is measured using simulations that output figures

of probability of bit error (or BER) versus E_b/N_0. First the modulation index to be used with the new optimum pulse shapes were approximated to some practical rational numbers that ease to reduce the receiver complexity by decreasing the number of phase states. Then an optimum CPM receiver based on phase trellis structure was used to see their optimal performances with these modulation indices. It has been shown that for the pulse shape with $L = 3$ choosing $h = 4/7$, and for the one with $L = 7$ choosing $h = 6/7$ result in very good error performances close to the optimum case. Then LD based receiver were used instead of optimum CPM receivers to see how the performance changes with complexity reduction applied. For $L = 3$ case, usage of only 2 matched filters instead of 56, and 14 states instead of 28 needed in the optimum case give the same performance. Even using 1 matched filter with 7 states has better performance than the modulation scheme used in GSM. For $L = 7$ case the results are more interesting. Using only 8 matched filters and 56 trellis states in an LD based receiver leads to a gain in power of 2.25dB, where it is computed to be 2.3dB for the optimum case in [5]. As a result, we can say that using LD based receivers which are based on the PAM representation of CPM signals give good results in error performance for the mentioned pulse shapes even after an acceptable complexity reduction is applied.

In this thesis, reduced-complexity Laurent Decomposition (LD) based receiver structures were considered for some particular optimum pulse shapes found in a previous work. Performance of the receivers were investigated only under AWGN channel. As a future work, performance in ISI channel, which is a more realistic case, may be investigated. Pulse optimization for practical modulation indices, like 4/7, 5/6 etc., may be considered to improve error performance for these cases. Further complexity reduction may be achieved by applying *reduced state sequence detection (RSSD)* method, [13], for phase states in addition to the method used in this work.

REFERENCES

[1] T. Aulin and Carl-Erik W. Sundberg, "Continuous Phase Modulation - Part I: Full Response Signaling", *IEEE Transactions On Commununications, vol. COM-29, pp. 196-209*, March 1981.

[2] T. Aulin, N. Rydbeck and Carl-Erik W. Sundberg, "Continuous Phase Modulation - Part II: Partial Response Signaling", *IEEE Transactions On Commununications, vol. COM-29, pp. 210-225*, March 1981.

[3] J. B. Anderson, T. Aulin and Carl-Erik W. Sundberg, "*Digital Phase Modulation*", Plenum Press, New York, 1986.

[4] J. G. Proakis, "*Digital Communications*", McGraw-Hill, New York, 2001.

[5] Ç. Enis Doyuran, "New Pulse Shapes For CPM Signals", *M.S. Thesis, Electrical and Electronics Engineering Department*, Middle East Technical University, Ankara, July 2001.

[6] Enis Doyuran, Yalcin Tanik, "New Pulse Shapes for CPM Signals", *Vehicular Technology Conference, 2006. VTC 2006-Spring. IEEE 63rd , vol.1, pp.236-240*, 7-10 May 2006.

[7] Pierre A. Laurent, "Exact And Approximate Construction Of Digital Phase Modulations By Superposition Of Amplitude Modulated Pulses (AMP)", *IEEE Transactions On Communications, vol. COM-34, No:2*, February 1986.

[8] U. Mengali, M. Moore, "Decomposition of Mary CPM Signals into PAM Waveforms", *IEEE Transactions On Information Theory, vol. 41, No:5*, September 1995.

[9] Erik Samuel Perrins, "Reduced Complexity Detection Methods For Continuous Phase Modulation", *Phd. Thesis, Department of Electrical and Computer Engineering*, Brigham Young University, Provo UT, December 2005.

[10] G. Kawas Kaleh, "Simple Coherent Receivers for Partial Response Continuous Phase Modulation", *IEEE Journal On Selected Areas In Communications, vol. 7, No:9*, December 1989.

[11] Yi Su, Shidong Zhou, "Performance Estimation of P State Coherent Binary CPM Receiver Based on Laurent Decomposition", *Wireless Communications, Networking and Mobile Computing, 2005. Proceedings. 2005 International Conference on , vol.1, pp. 573-578*, 23-26 September 2005.

[12] Marvin K. Simon, Mohamed-Slim Alouini, "*Digital Communication over Fading Channels*", John Wiley & Sons, Inc., New Jersey, 2005.

[13] A. Svensson, "Reduced State Sequence Detection of Partial Response Continuous Phase Modulation", *IEEE Proceedings, part I, vol. 138, pp. 256-268*, August 1991.

[14] W. Tang, E. Shwedyk, "A Quasi-Optimum Receiver for Continuous Phase Modulation", *IEEE Transactions on Communications, vol. 48, pp. 1087-1090*, July 2000.

[15] T. Aulin C.-E. W. Sundberg, "An Easy Way to Calculate Power Spectra for Digital FM", *IEEE Proceedings, vol. 130, p. 519-526*, October 1983.

[16] J. Huber, W. Liu, "An Alternative Approach to Reduced Complexity CPM Receivers", *IEEE Journal on Selected Areas in Communications, vol. 7, pp. 1427-1436*, December 1989.

[17] A. Svensson, C.-E. Sundberg, and T. Aulin, "A Class of Reduced-Complexity Viterbi Detectors for Partial Response Continuous Phase Modulation", *IEEE Transactions on Communications, vol. 32, pp. 1079-1087*, October 1984.

[18] S. J. Simmons, "Simplified Coherent Detection of CPM", *IEEE Transactions on Communications, vol. 43, pp. 726-728*, FebruayMarchApril 1995.

[19] S. J. Simmons, P. H. Wittke, "Low Complexity Decoders for Constant Envelope Digital Modulations", *IEEE Transactions on Communications, vol. 31, pp. 1273-1280*, December 1983.

[20] GSM 05.05 (ETS 300 577), "Digital Cellular Telecommunications System (Phase 2); Radio Transmission and Reception", *ETSI*, November 1997

[21] Simon Haykin, "*Communication Systems* - 4^{th} *Edition*", John Wiley & Sons, Inc., New Jersey, 2001.

[22] O. Dural, J. G. Proakis, "The Performance of Simplified Maximum-Likelihood Sequence Detector for Continuous Phase Modulation Scheme", *IEEE International Conference on Communications, ICC 2000, vol. 2, pp. 641-645*, 2000.